Correlation between v_n and p_T in Pb+Pb and Xe+Xe collisions with ATLAS

ATLAS-CONF-2021-001

Poster by Somadutta Bhatta, Tuesday 12th

Arabinda Behera

For the ATLAS Collaboration

12th January, 2021

Stony Brook University

ATLAS EXPERIMENT

v_n - [p_T] Correlation

- In HIC - collision overlap has shape and size

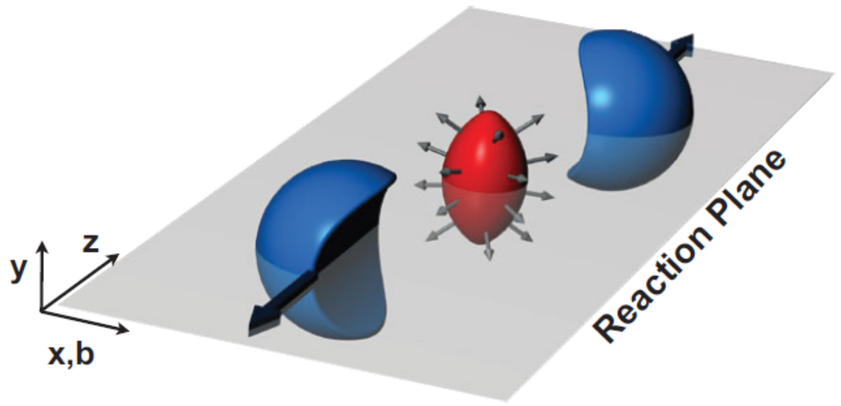

- Size → radial flow - avg. momentum

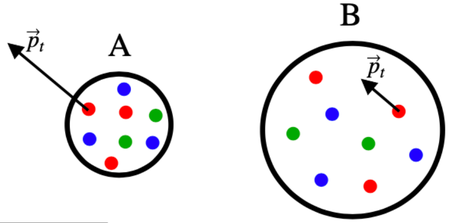

$$1/R \longrightarrow [p_T]$$

$$\boxed{S_A = S_B \quad R_A < R_B} \Longrightarrow \boxed{T_A > T_B} \Longrightarrow \boxed{\langle p_t \rangle_A > \langle p_t \rangle_B}$$

- Shape → anisotropic flow

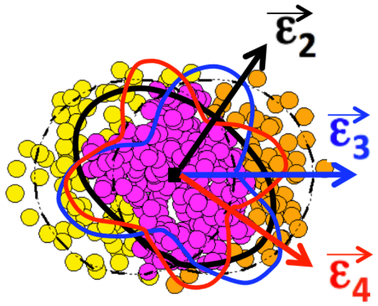

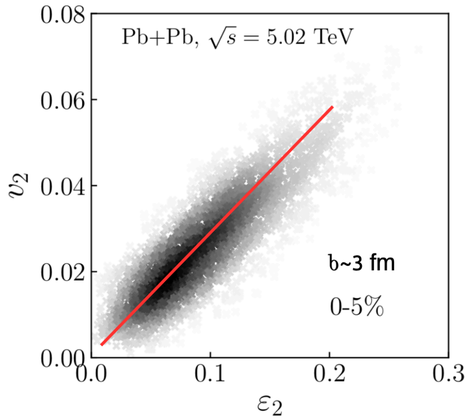

$$v_n \propto \epsilon_n$$

- Initial State - correlation and fluctuations of shape and size
- **Final State - correlation between v_n and [p_T]**

v_n - $[p_T]$ Correlation

- In HIC - collision overlap has shape and size

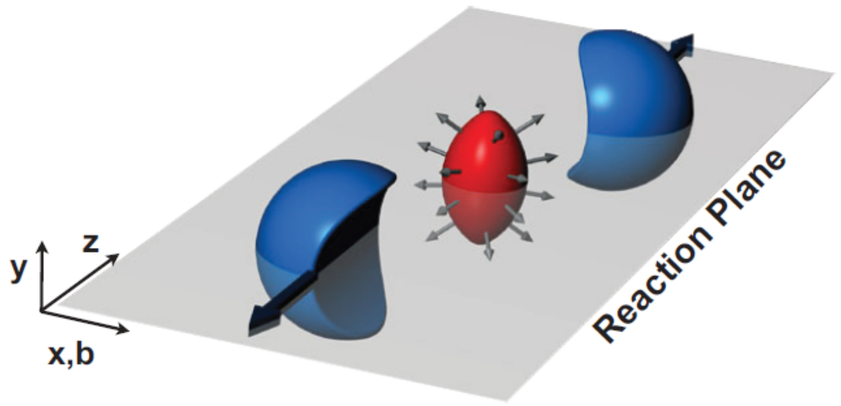

- Size → radial flow - avg. momentum

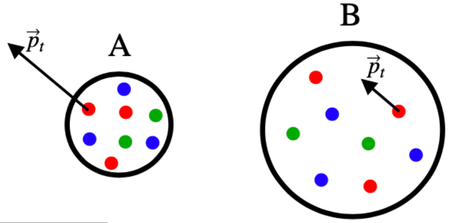

$$1/R \longrightarrow [p_T]$$

$$\boxed{\begin{matrix} S_A = S_B \\ R_A < R_B \end{matrix}} \Longrightarrow \boxed{T_A > T_B} \Longrightarrow \boxed{\langle p_t \rangle_A > \langle p_t \rangle_B}$$

- Shape → anisotropic flow

arXiv:2101.00168

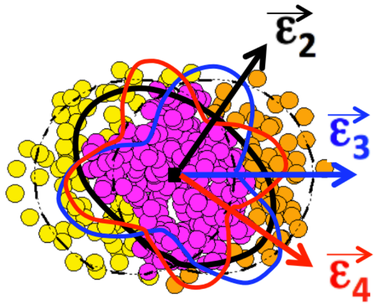

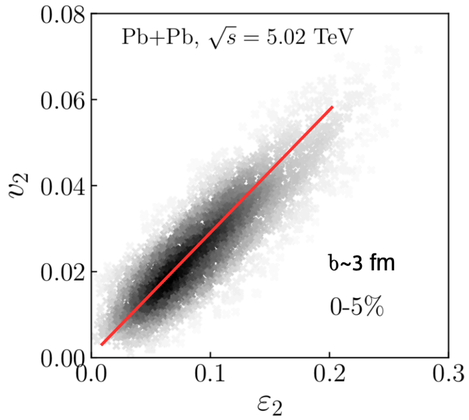

$$v_n \propto \epsilon_n$$

- Pearson's correlation coefficient

$$\rho(v_n^2, [p_T]) = \frac{cov(v_n^2, [p_T])}{\sqrt{var(v_n^2)}\sqrt{var([p_T])}}$$

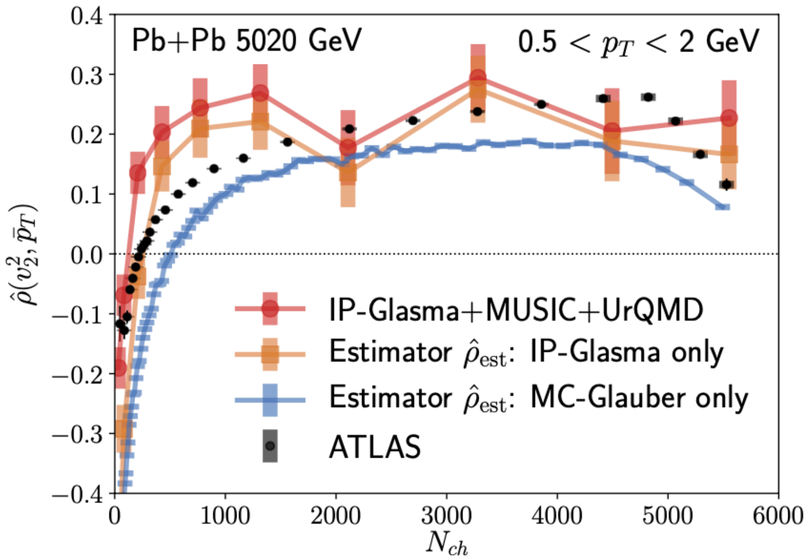

Eur. Phys. J. C 79 (2019) 985

Phys. Rev. C 102, 034905 (2020)

- Initial State - correlation and fluctuations of shape and size
- **Final State - correlation between v_n and $[p_T]$**

v_n - [p_T] Correlation

- Nuclear deformation

$$D_{WS}(r) = \frac{D_0}{1 + e^{(r - R_0(1+\beta Y_{20}))/a}}$$

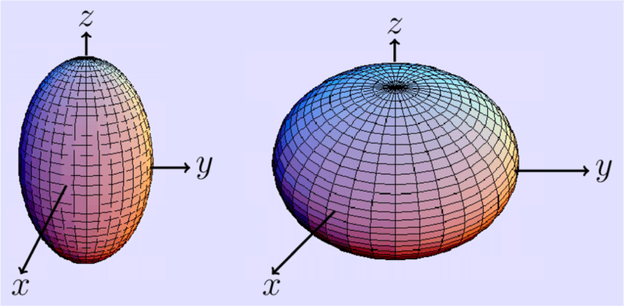

β > 0 Prolate β < 0 Oblate

- LHC - Pb+Pb (β ≃ 0) , Xe+Xe (β ≃ 0.16)

- Trento results
  - Smaller ρ_2 in Xe+Xe than Pb+Pb
  - Deformation lowers ρ_2 in the central region

Phys. Rev. C 102, 024901 (2020)

G. Giacalone

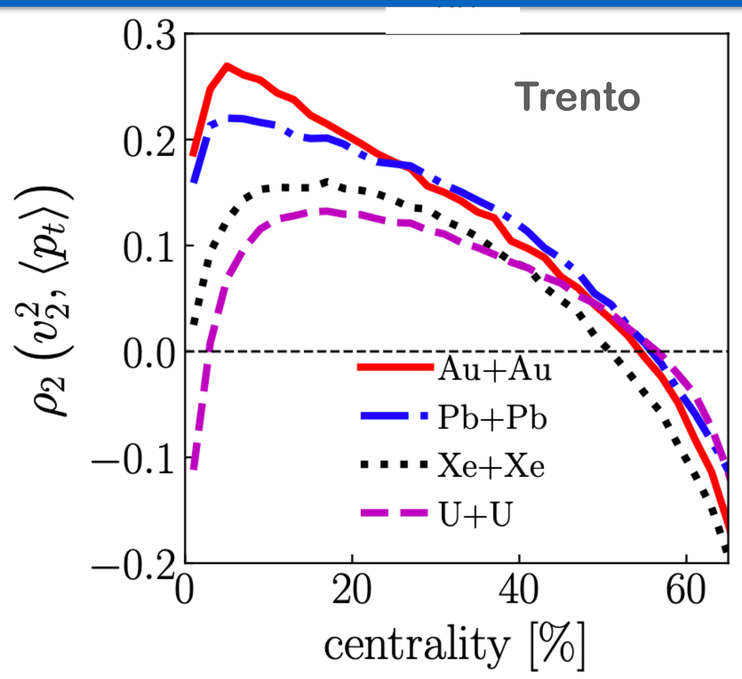

v_n - [p_T] Correlation

- Nuclear deformation

$$D_{WS}(r) = \frac{D_0}{1 + e^{(r - R_0(1+\beta Y_{20}))/a}}$$

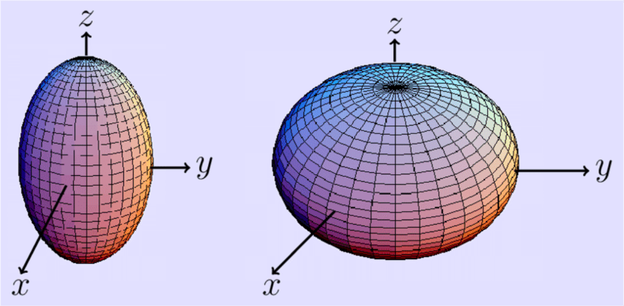

β > 0 Prolate β < 0 Oblate

- LHC - Pb+Pb (β ≃ 0) , Xe+Xe (β ≃ 0.16)

- Trento results
  - Smaller ρ_2 in Xe+Xe than Pb+Pb
  - Deformation lowers ρ_2 in the central region

Phys. Rev. C 102, 024901 (2020)

G. Giacalone

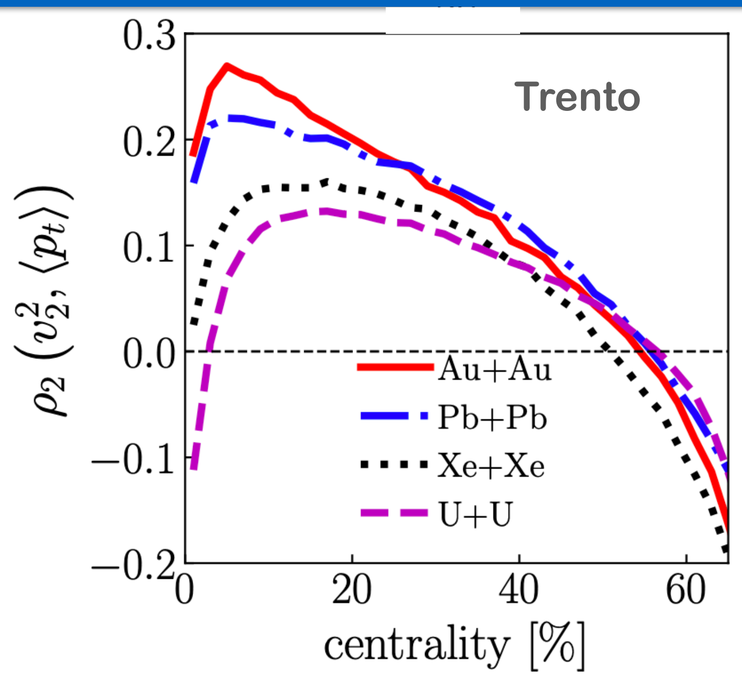

- Centrality fluctuations
  - Smearing between N_{part} and N_{ch}

Same N_{part} - different N_{ch}

Same N_{ch} - different N_{part}

$$p(Obs.|N_{ch}) = \sum_{cent} p(Obs.|cent) \otimes p(cent|N_{ch})$$

Phys. Rev. Research 2, 023319 (2020)

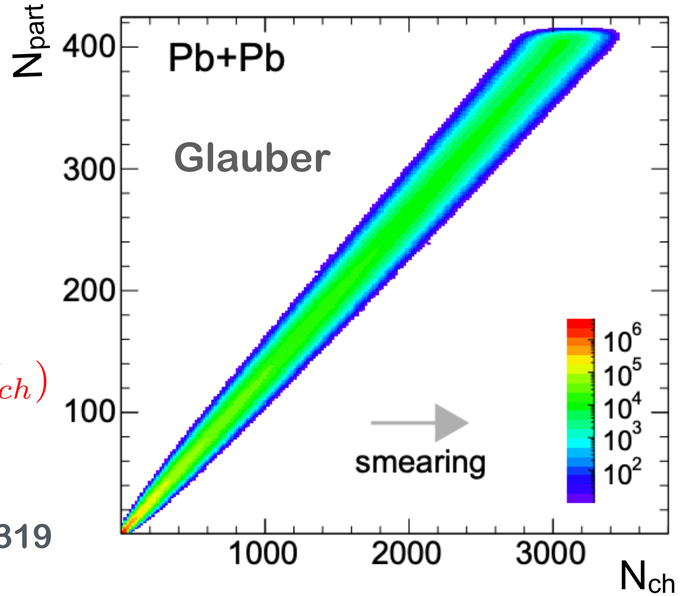

v_n - [p_T] Correlation

- Nuclear deformation

$$D_{WS}(r) = \frac{D_0}{1 + e^{(r - R_0(1+\beta Y_{20}))/a}}$$

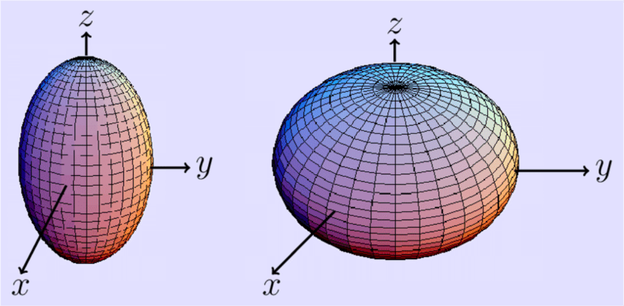

β > 0 Prolate β < 0 Oblate

- LHC - Pb+Pb (β ≃ 0) , Xe+Xe (β ≃ 0.16)

v_n - [p_T] Correlation - Pb+Pb vs Xe+Xe

- System-size dependence
- Centrality fluctuation
- Deformation effects

- Trento results
  - Smaller ρ_2 in Xe+Xe than Pb+Pb
  - Deformation lowers ρ_2 in the central region

Phys. Rev. C 102, 024901 (2020)

G. Giacalone

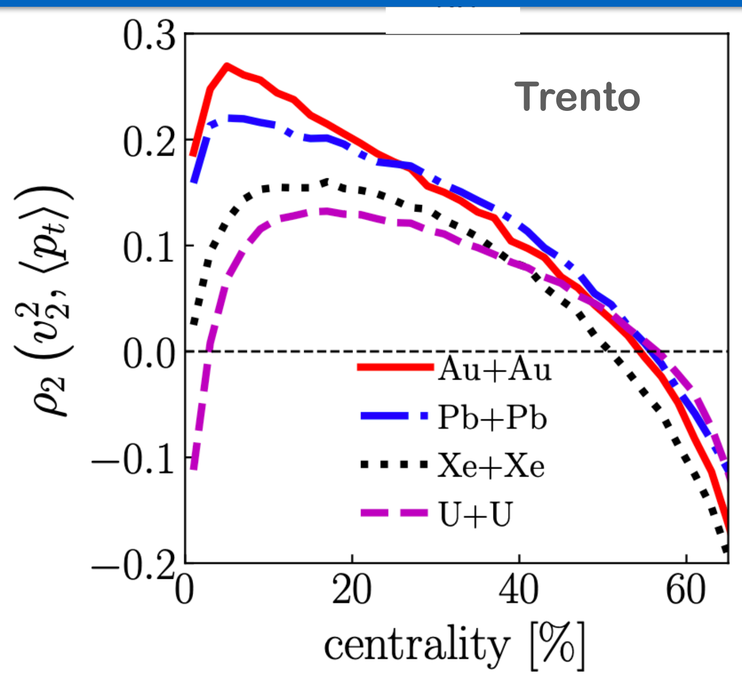

- Centrality fluctuations
  - Smearing between N_{part} and N_{ch}

Same N_{part} - different N_{ch}

Same N_{ch} - different N_{part}

$$p(Obs.|N_{ch}) = \sum_{cent} p(Obs.|cent) \otimes p(cent|N_{ch})$$

Phys. Rev. Research 2, 023319 (2020)

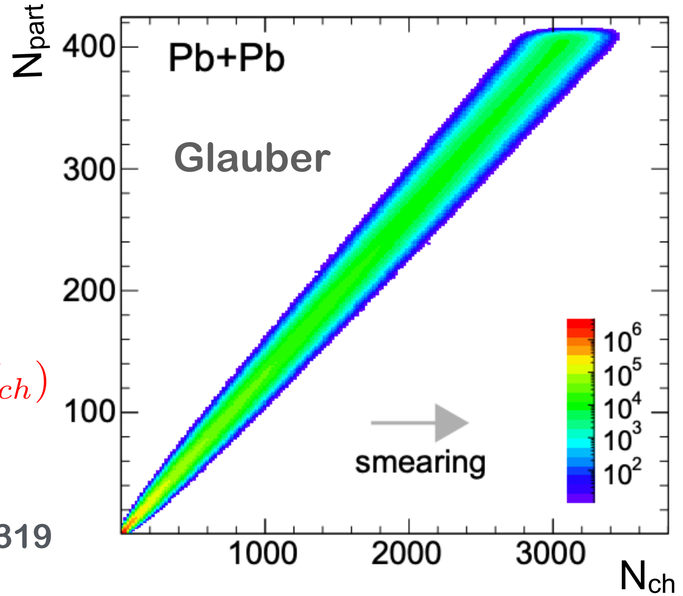

Observable

- Pearson's Correlation Coefficient

Phys. Rev. C 93, 044908 (2016)

$$cov(v_n^2, [p_T]) = \langle\langle e^{in(\phi_i - \phi_j)}(p_{T,k} - \langle[p_T]\rangle)\rangle\rangle_{ev}$$

$$\rho(v_n^2, [p_T]) = \frac{cov(v_n^2, [p_T])}{\sqrt{var(v_n^2)}\sqrt{c_k}}$$

$$c_k = \langle\langle(p_{T,i} - \langle[p_T]\rangle)(p_{T,j} - \langle[p_T]\rangle)\rangle\rangle_{ev}$$

$$var(v_n^2) = v_n\{2\}^4 - v_n\{4\}^4$$
$$= \langle\langle e^{in(\phi_i + \phi_k - \phi_j - \phi_l)}\rangle\rangle_{ev} - \langle\langle e^{in(\phi_i - \phi_j)}\rangle\rangle_{ev}^2$$

- cov (v_n^2,[p_T]) - triplet of particles
  - Standard, two-subevent and three-subevent methods
  - Subevent methods can suppress non-flow

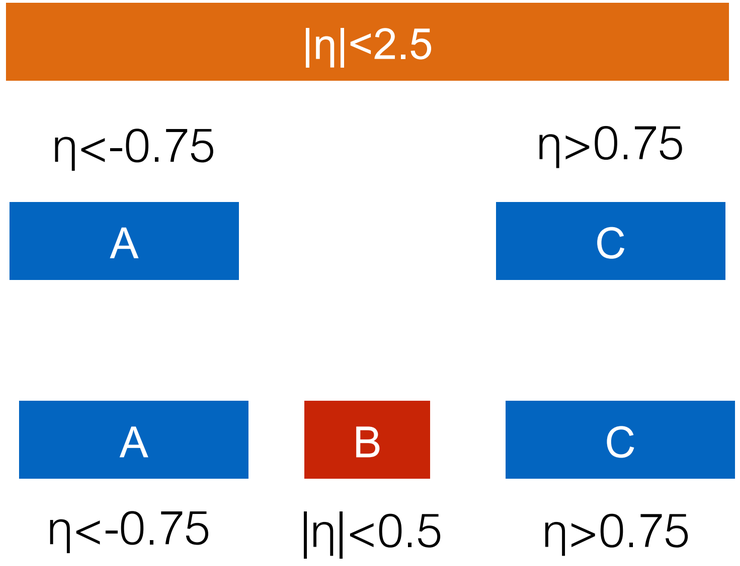

Comparison of cov(v_n^2,[p_T]) - subevents methods

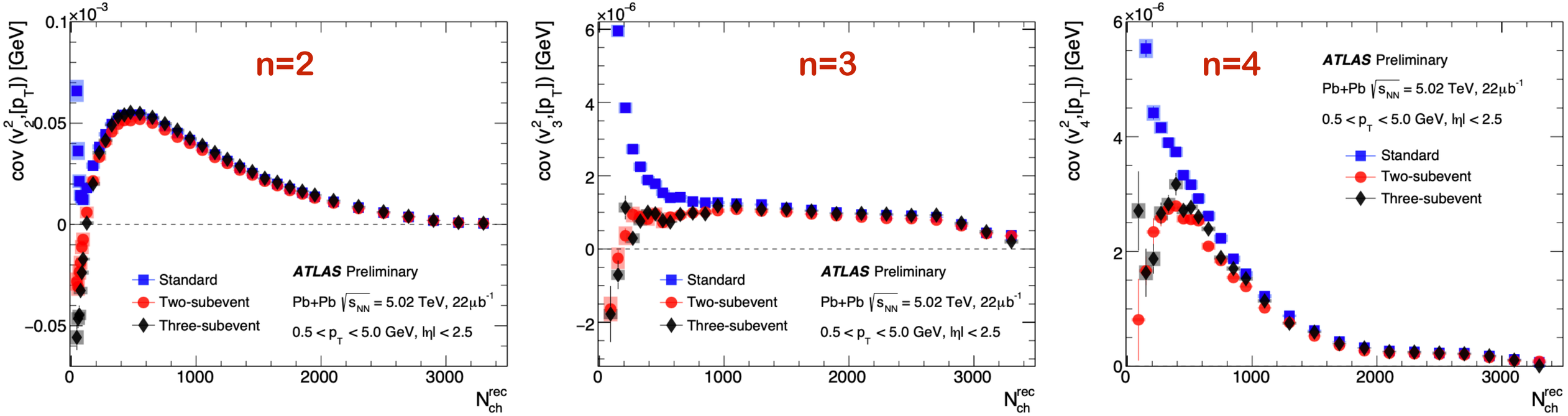

$$\rho(v_n^2, [p_T]) = \frac{cov(v_n^2, [p_T])}{\sqrt{var(v_n^2)}\sqrt{c_k}}$$

- Non-flow significant in standard method at low N_{ch}
- Difference between subevent methods are expected
  - different in [p_T] and v_n along η
  - different decorrelation of v_n and [p_T] along Δη
- Combined-subevent method - final results are average of two- and three-subevent methods

Results

Focus on v_2 and v_3 results

v_4 results in backup slides

Variances of v_n and $[p_T]$

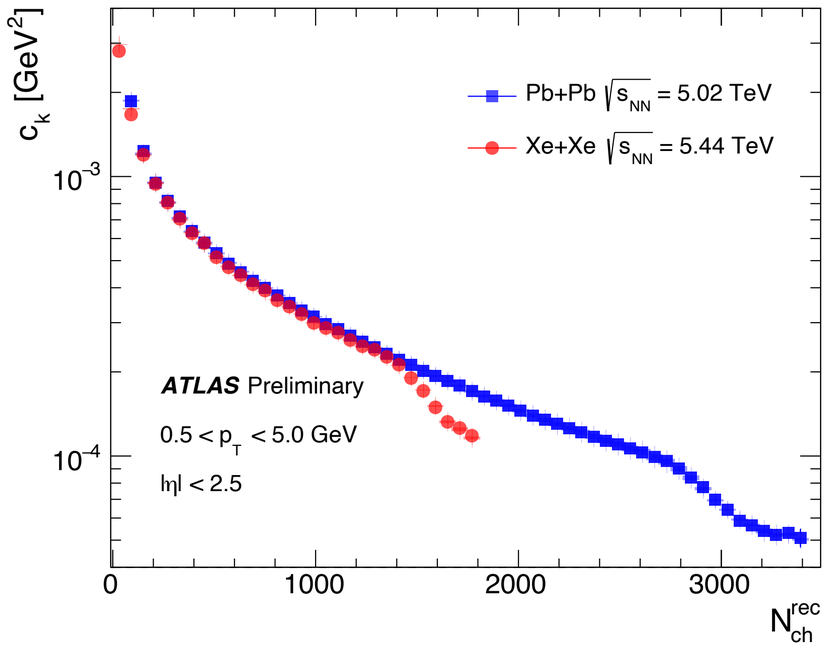

- c_k follows common power-law in Pb+Pb and Xe+Xe

$$\rho(v_n^2, [p_T]) = \frac{cov(v_n^2, [p_T])}{\sqrt{var(v_n^2)}\sqrt{c_k}}$$

Variances of v_n and $[p_T]$

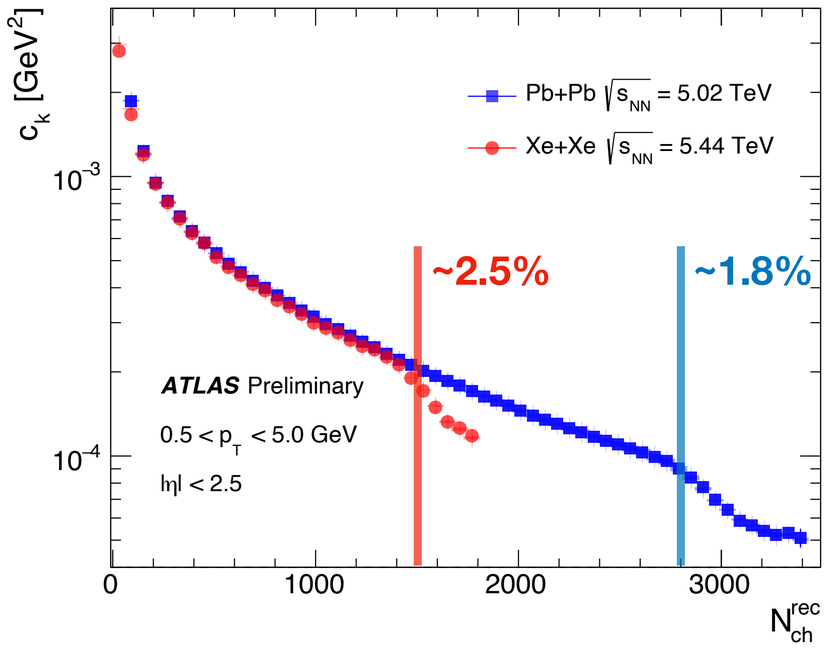

- c_k follows common power-law in Pb+Pb and Xe+Xe
- Departure from power-law in ultra central region - due to upper boundary effect

$$\rho(v_n^2, [p_T]) = \frac{cov(v_n^2, [p_T])}{\sqrt{var(v_n^2)}\sqrt{c_k}}$$

Variances of v_n and $[p_T]$

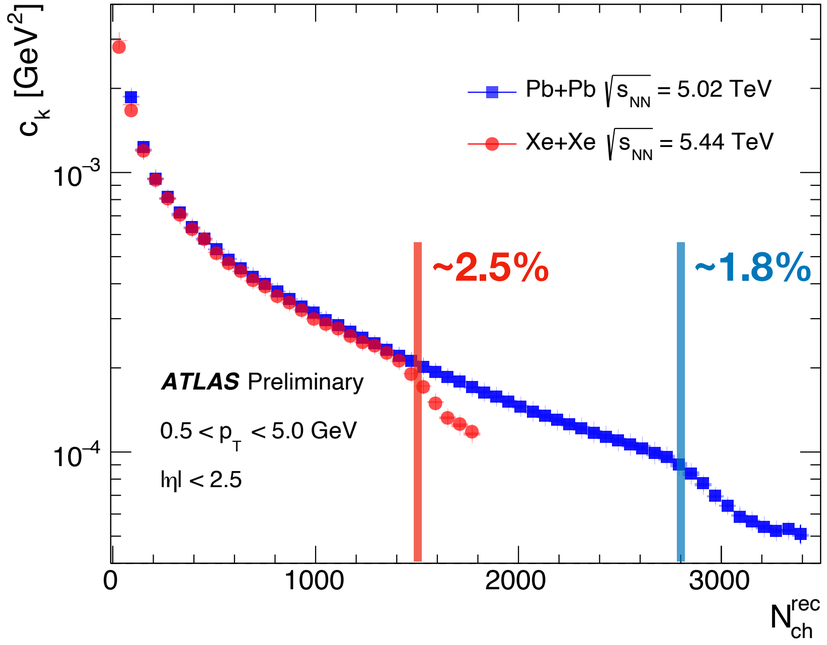

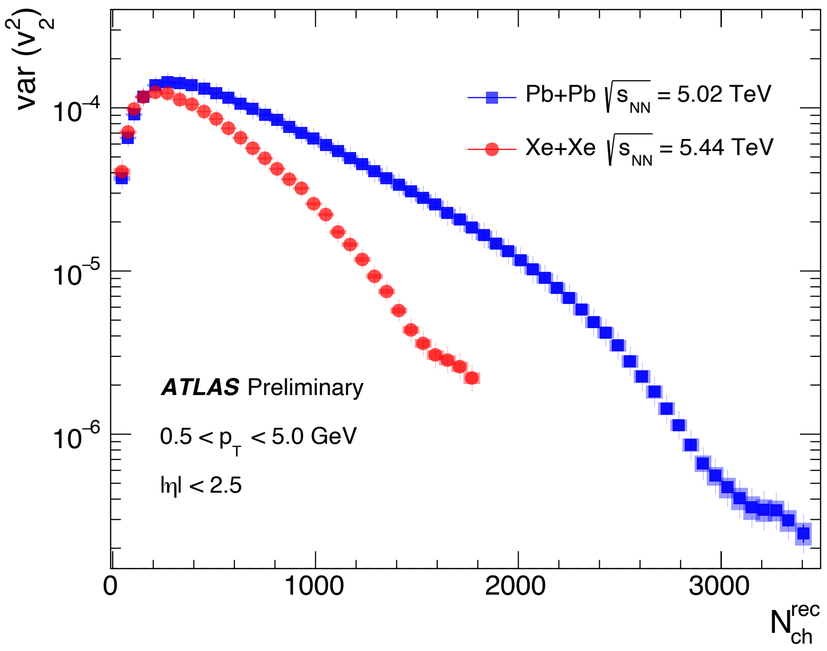

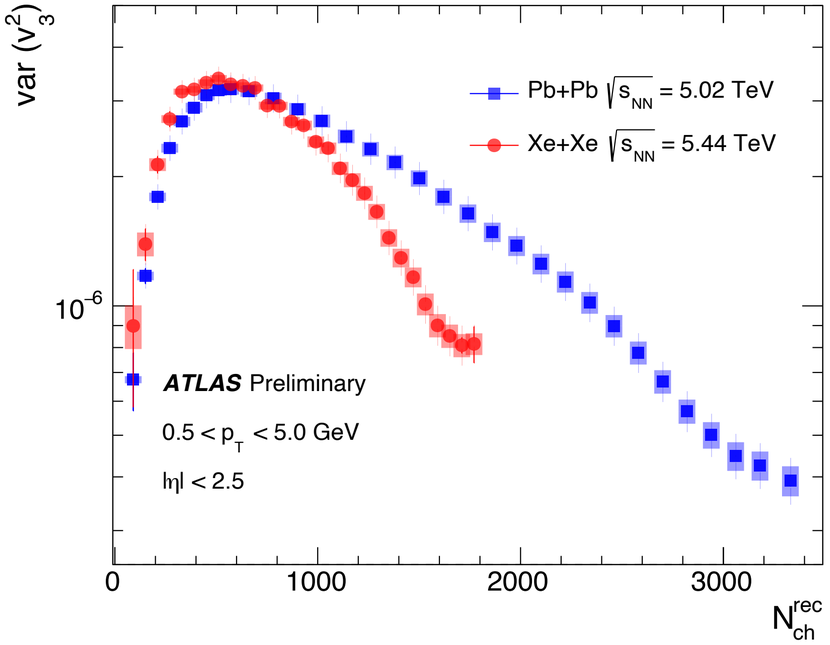

- c_k follows common power-law in Pb+Pb and Xe+Xe
- Departure from power-law in ultra central region - due to upper boundary effect

$$\rho(v_n^2, [p_T]) = \frac{cov(v_n^2, [p_T])}{\sqrt{var(v_n^2)}\sqrt{c_k}}$$

- var(v_n^2) follows similar N_{ch} dependence in both system
- The ordering and trends are similar to v_n

Phys. Rev. C 101 (2020), 024906

Variances of v_n and $[p_T]$

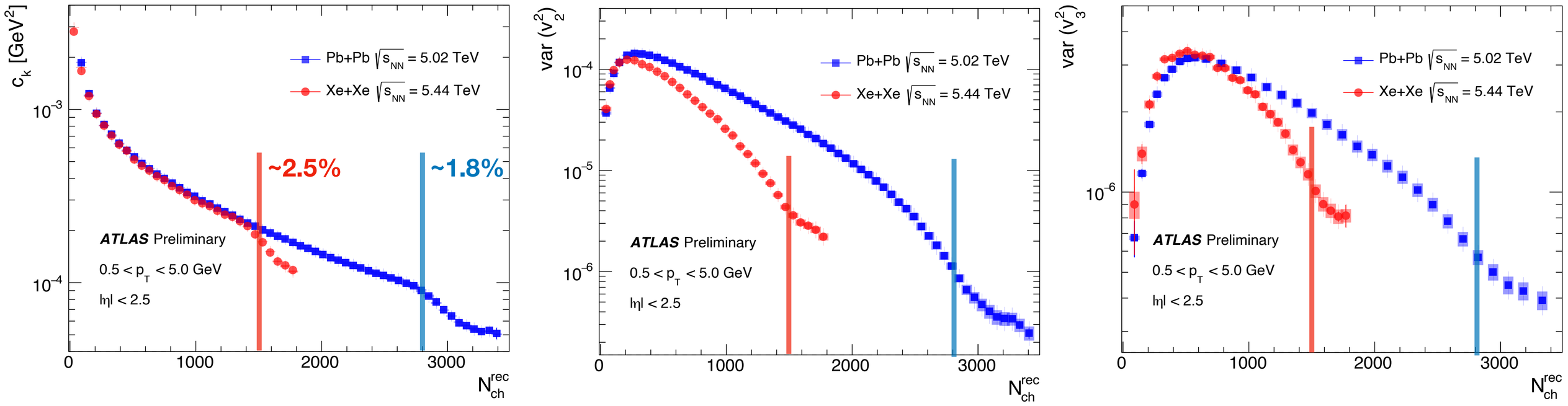

- c_k follows common power-law in Pb+Pb and Xe+Xe
- Departure from power-law in ultra central region - due to upper boundary effect

$$\rho(v_n^2, [p_T]) = \frac{cov(v_n^2, [p_T])}{\sqrt{var(v_n^2)}\sqrt{c_k}}$$

- var(v_n^2) follows similar N_{ch} dependence in both system
- The ordering and trends are similar to v_n

Phys. Rev. C 101 (2020), 024906

- var(v_n^2) shows some upper boundary effects

Comparisons - Pb+Pb vs Xe+Xe

$$\rho(v_n^2, [p_T]) = \frac{cov(v_n^2, [p_T])}{\sqrt{var(v_n^2)}\sqrt{c_k}}$$

- As a function of N_{ch}
  - Low N_{ch} - similar values
  - High N_{ch} - Opposite ordering between n=2 and n=3

$$\rho_2^{Xe+Xe} < \rho_2^{Pb+Pb}$$

$$\rho_3^{Xe+Xe} > \rho_3^{Pb+Pb}$$

N_{ch} (size)

n=2

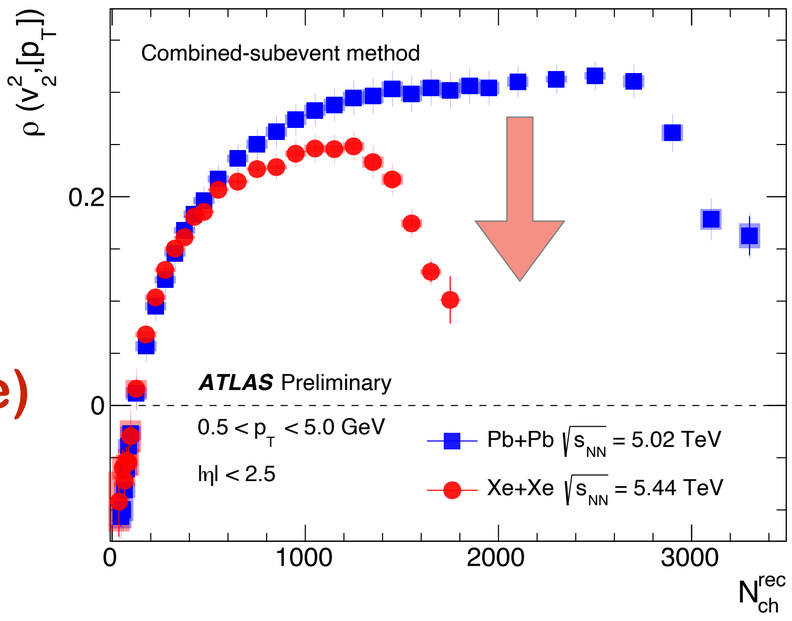

n=3

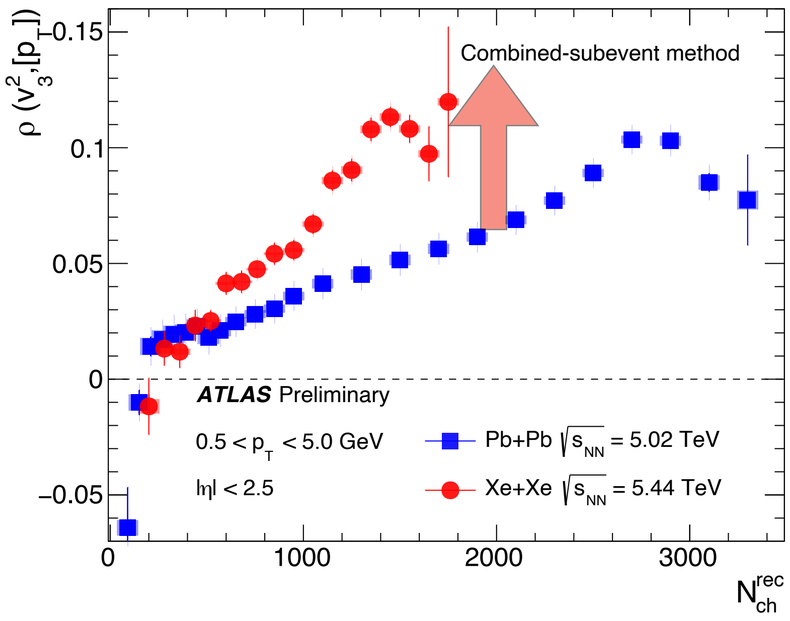

Comparisons - Pb+Pb vs Xe+Xe

$$\rho(v_n^2, [p_T]) = \frac{cov(v_n^2, [p_T])}{\sqrt{var(v_n^2)}\sqrt{c_k}}$$

- As a function of N_{ch}
  - Low N_{ch} - similar values
  - High N_{ch} - Opposite ordering between n=2 and n=3

$$\rho_2^{Xe+Xe} < \rho_2^{Pb+Pb}$$

$$\rho_3^{Xe+Xe} > \rho_3^{Pb+Pb}$$

- As a function of centrality
  - ρ_{v_2} is smaller in Xe+Xe
  - but ρ_{v_3} is comparable

n=2 **n=3**

N_{ch} (size)

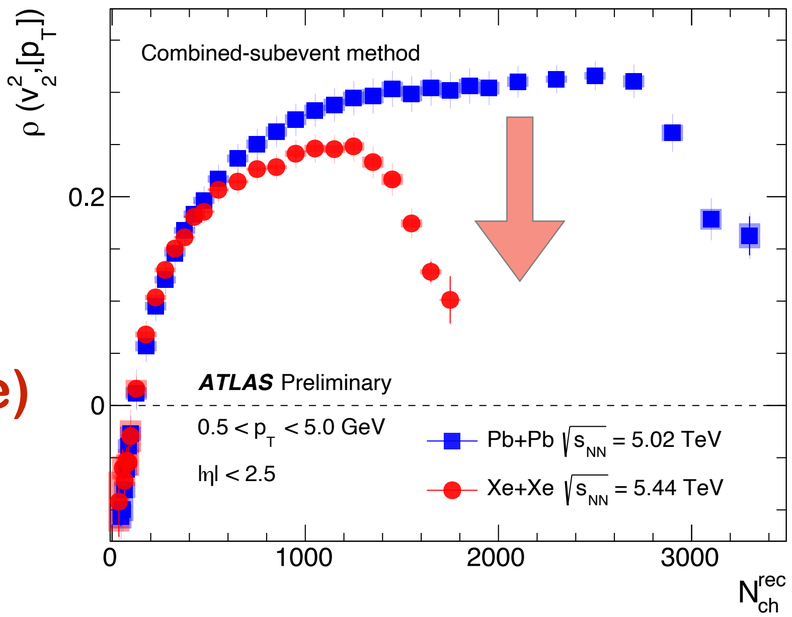

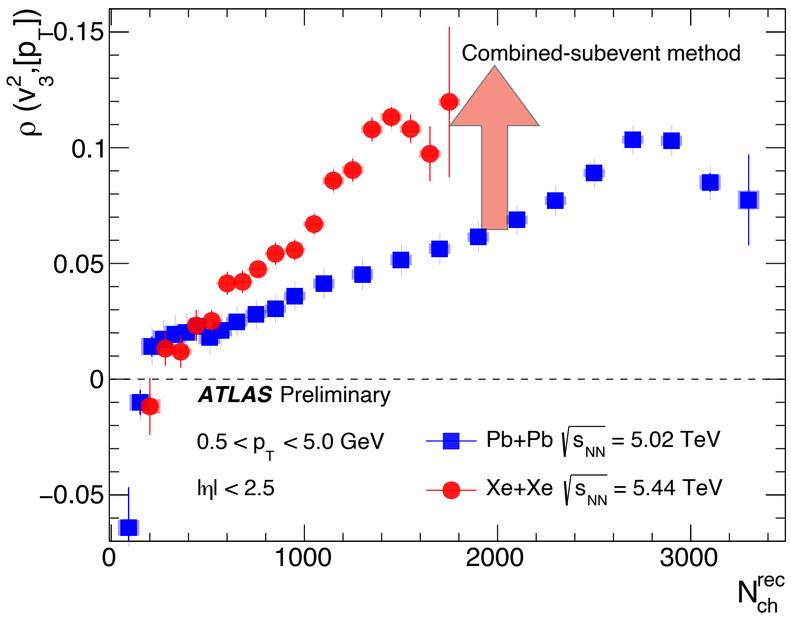

Cent (shape)

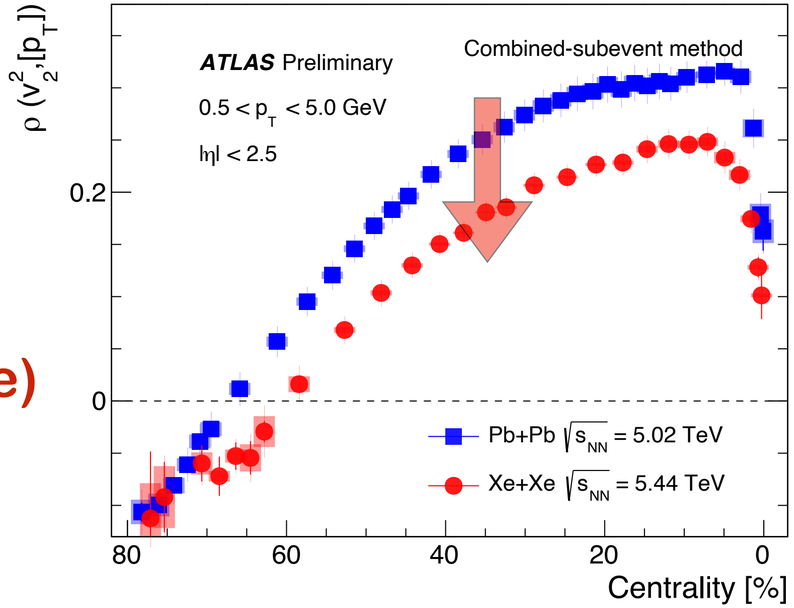

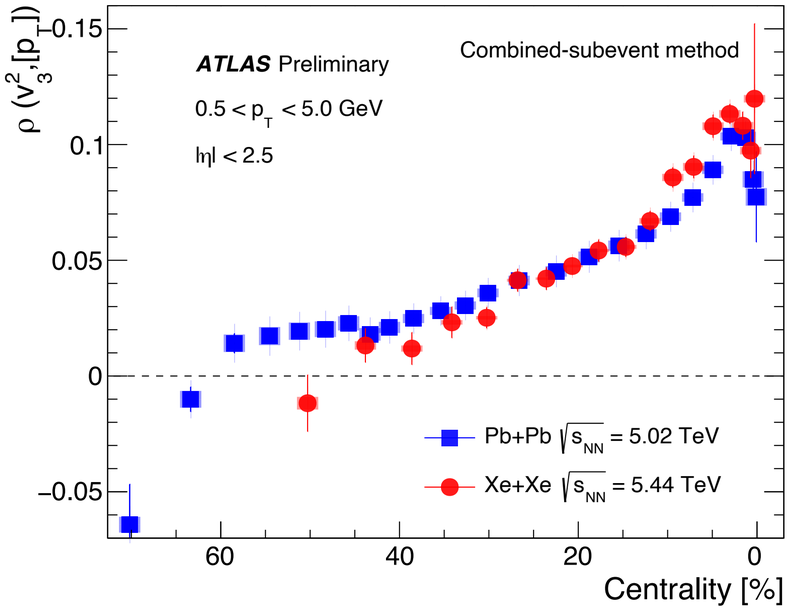

Dependence on p_T range

- In both systems ρ is larger for $0.5< p_T <5.0$ GeV than $0.5< p_T <2.0$ GeV - increase due to high p_T particles

- In Xe+Xe : ρ is consistent for $0.5< p_T <2.0$ GeV and $0.3< p_T <2.0$ GeV

- Low p_T region well described by hydrodynamics - little effect to more low-p_T particles

n=2 n=3

Pb+Pb

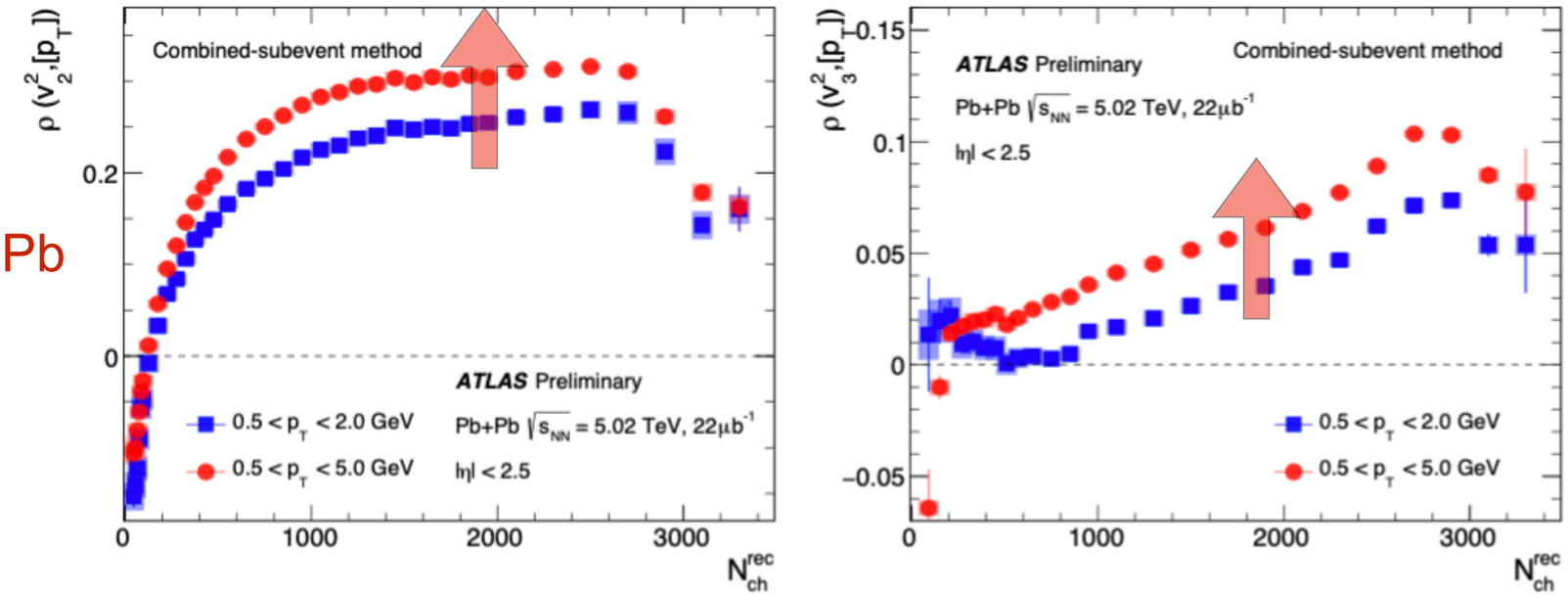

Xe+Xe

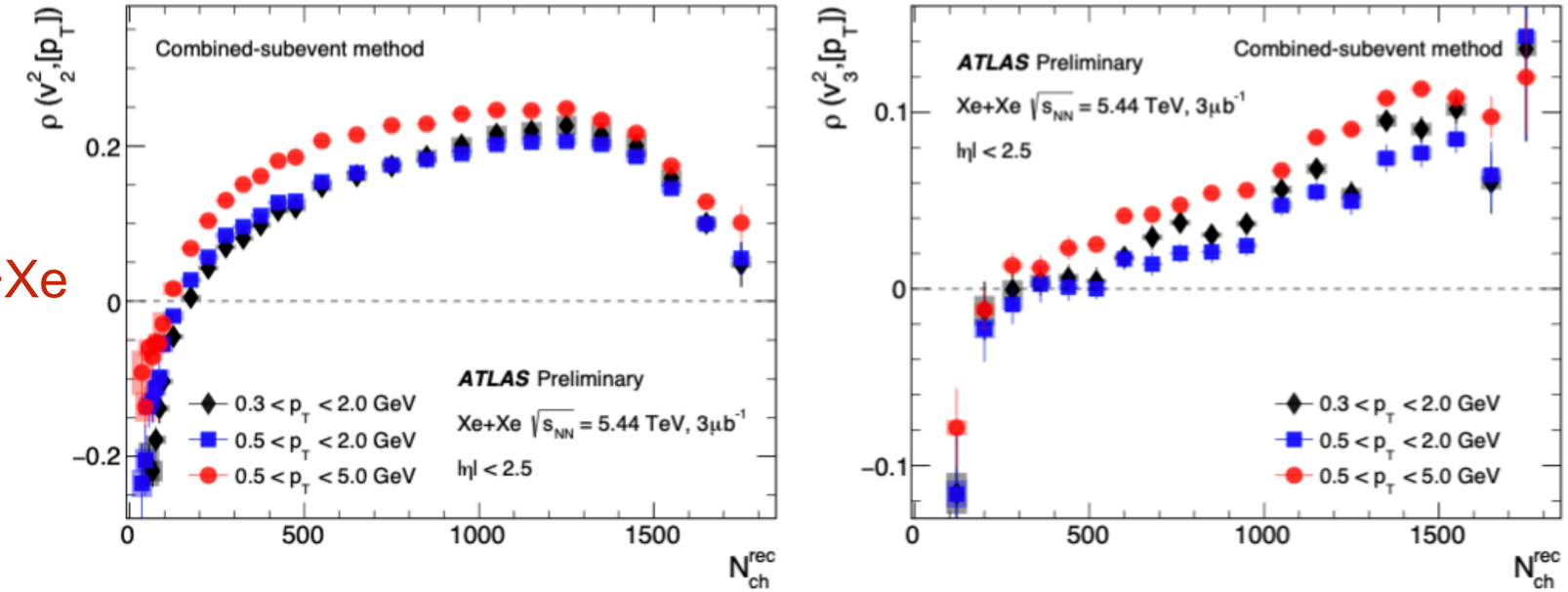

Dependence on η-range (Pb+Pb)

- Two eta ranges compared

$$|\eta| < 2.5 \qquad |\eta| < 1.0$$

A : η < -0.35 | B : |η| < 0.3 | C : η > 0.35

- c_k is larger by 10% for |η| < 1
- var(v_n^2) is larger by 10-20% for |η| < 1
- Reasons
  - The v_n and [p_T] magnitudes are larger for |η| < 1
  - Decorrelation smaller for |η| < 1

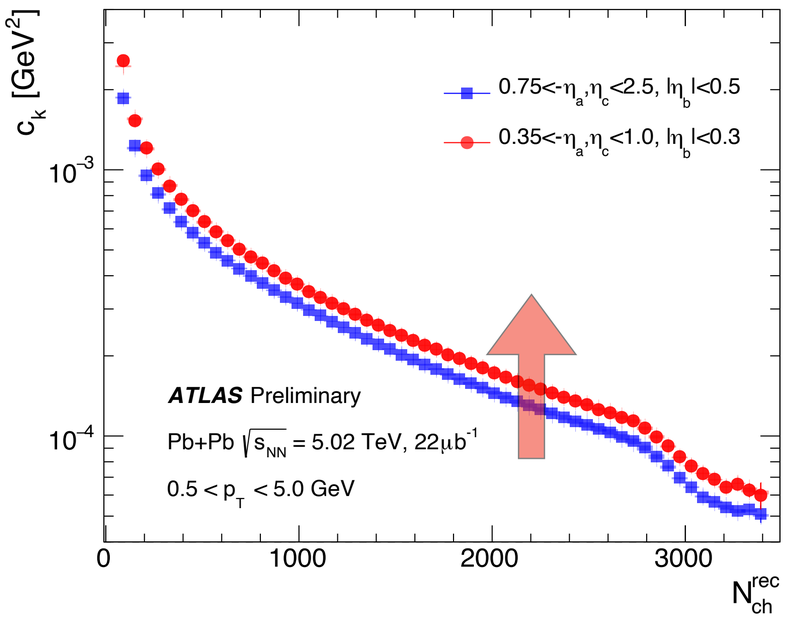

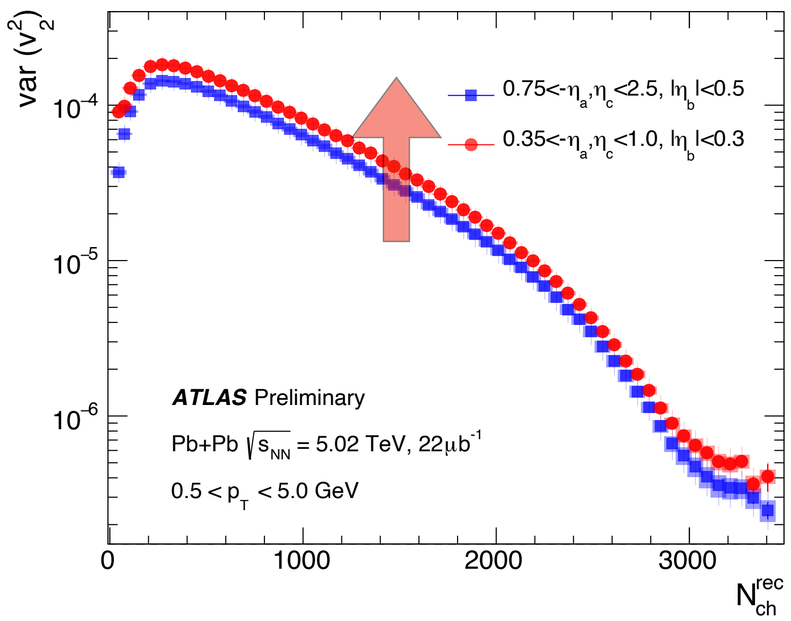

Dependence on η-range (Pb+Pb)

- Two eta ranges compared

$$|\eta| < 2.5 \qquad |\eta| < 1.0$$

A : η < -0.35 | B : |η| < 0.3 | C : η > 0.35

- c_k is larger by 10% for |η| < 1
- var(v_n^2) is larger by 10-20% for |η| < 1
- Reasons
  - The v_n and [p_T] magnitudes are larger for |η| < 1
  - Decorrelation smaller for |η| < 1
- Covariances show good agreement between η-ranges
- ρ_{v_n} are systematically smaller for |η| < 1 due to smaller c_k and var(v_n^2)

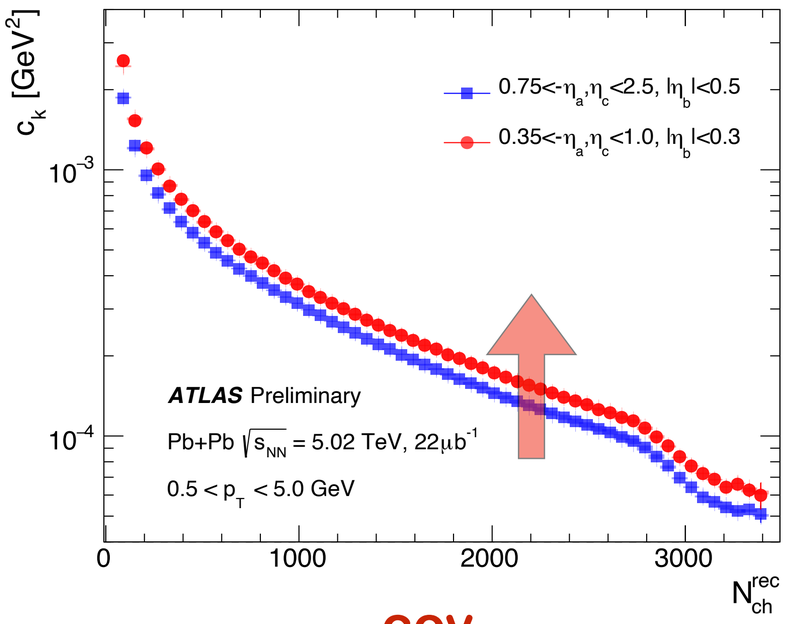

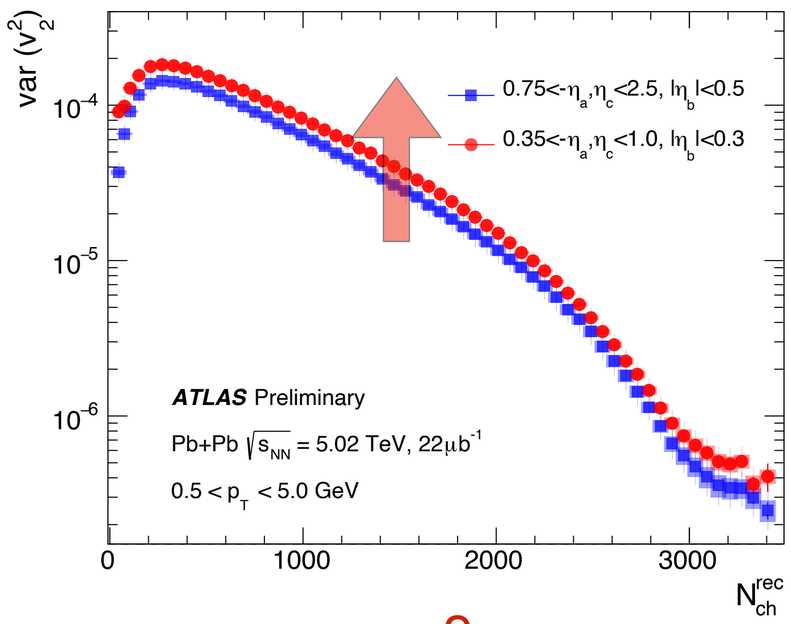

cov

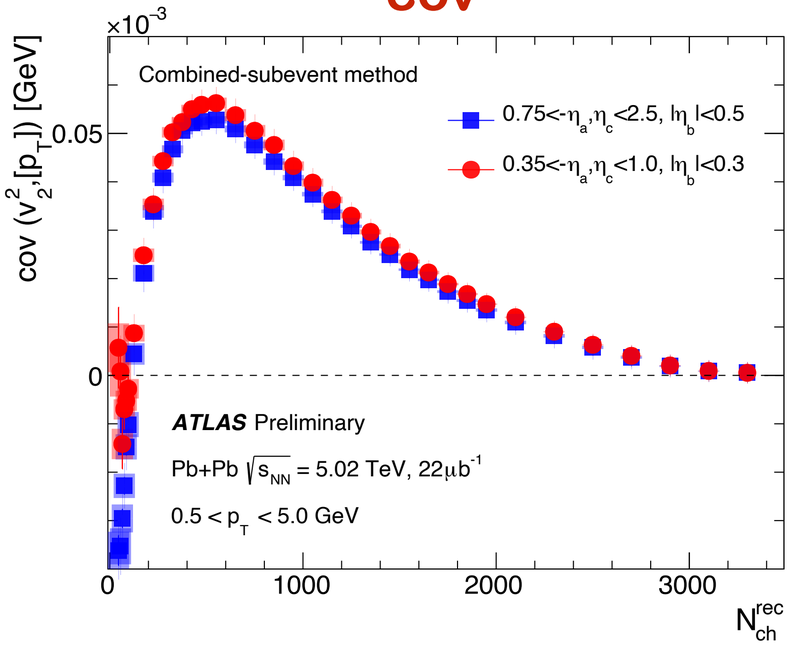

ρ

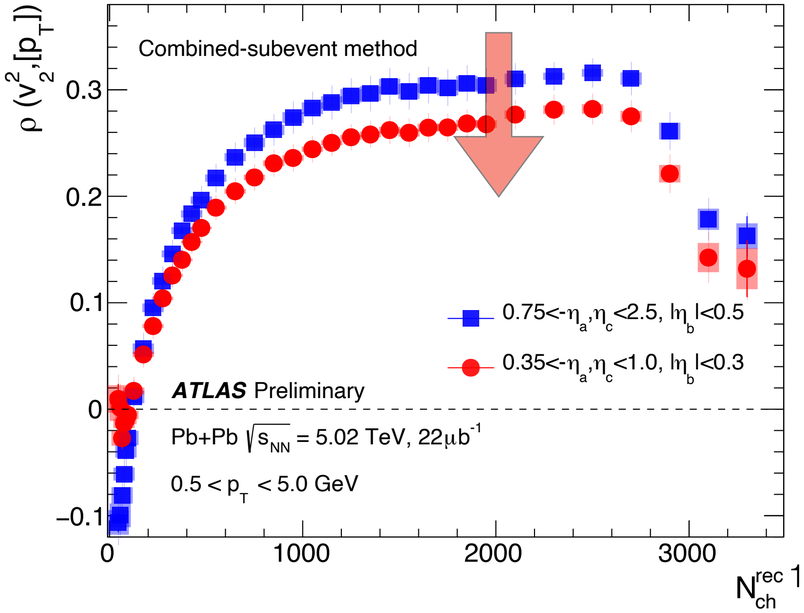

Centrality fluctuations in v_n

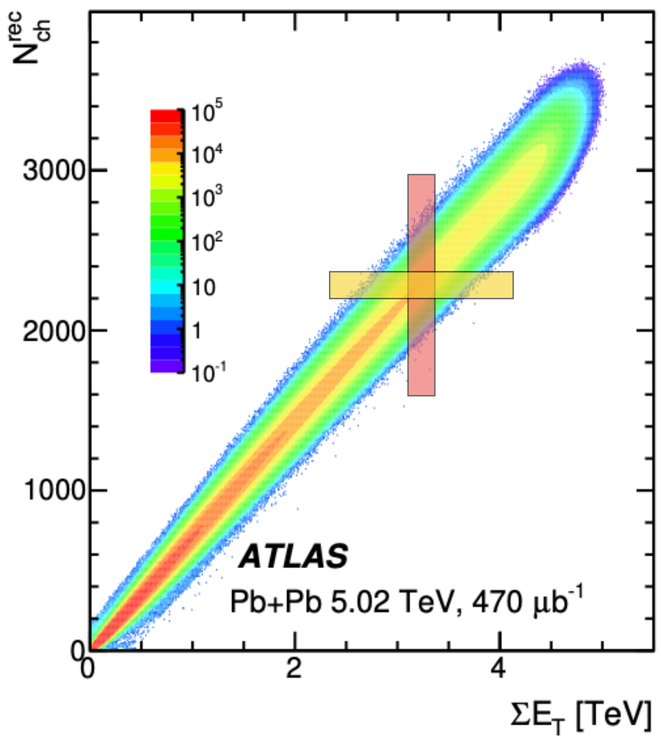

JHEP 01 (2020) 51

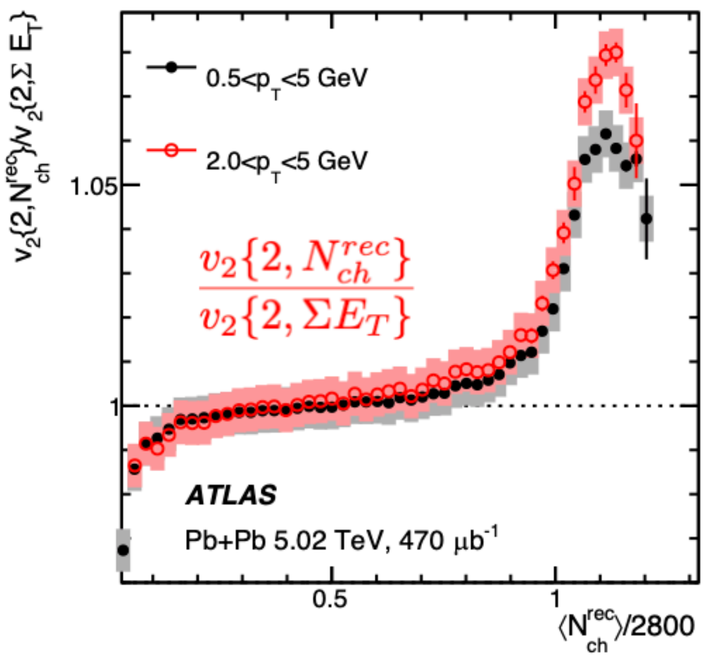

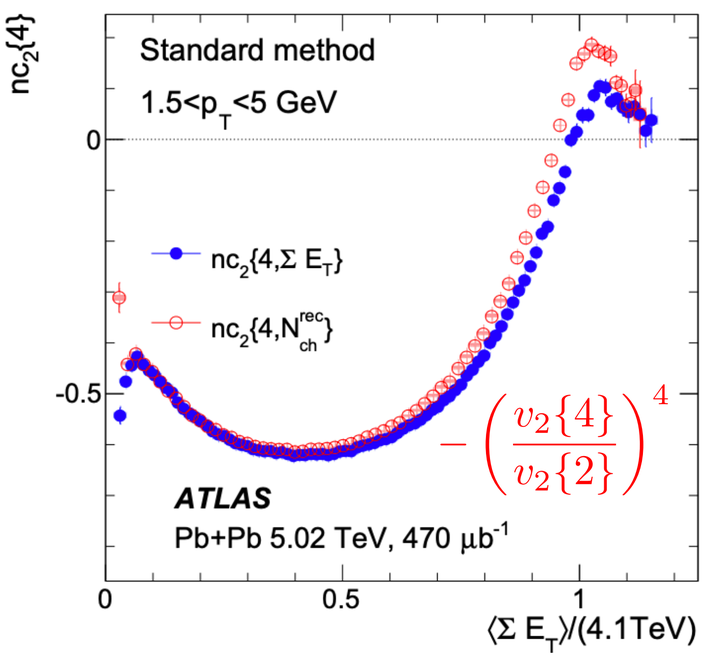

$$p(Obs.|N_{ch}) = \sum_{cent} p(Obs.|cent) \otimes p(cent|N_{ch})$$

- True centrality unknown
- Smearing between N_{ch} and E_T - Same N_{ch} but different E_T, Same E_T but different N_{ch}
- Event averaging in N_{ch} and E_T bins - centrality fluctuations

- Centrality fluctuation - large effect for $v_2\{2\}$ in central region
- Larger centrality fluctuation effect for higher particle-cumulants
- Effect present in much broader centrality range for both n=2 and n=3

Centrality fluctuations in v_n-[p_T] correlation

- E_T and N_{ch} are mapped to centrality (based on E_T cuts)
- Significantly large centrality fluctuations in central and peripheral

Pb+Pb

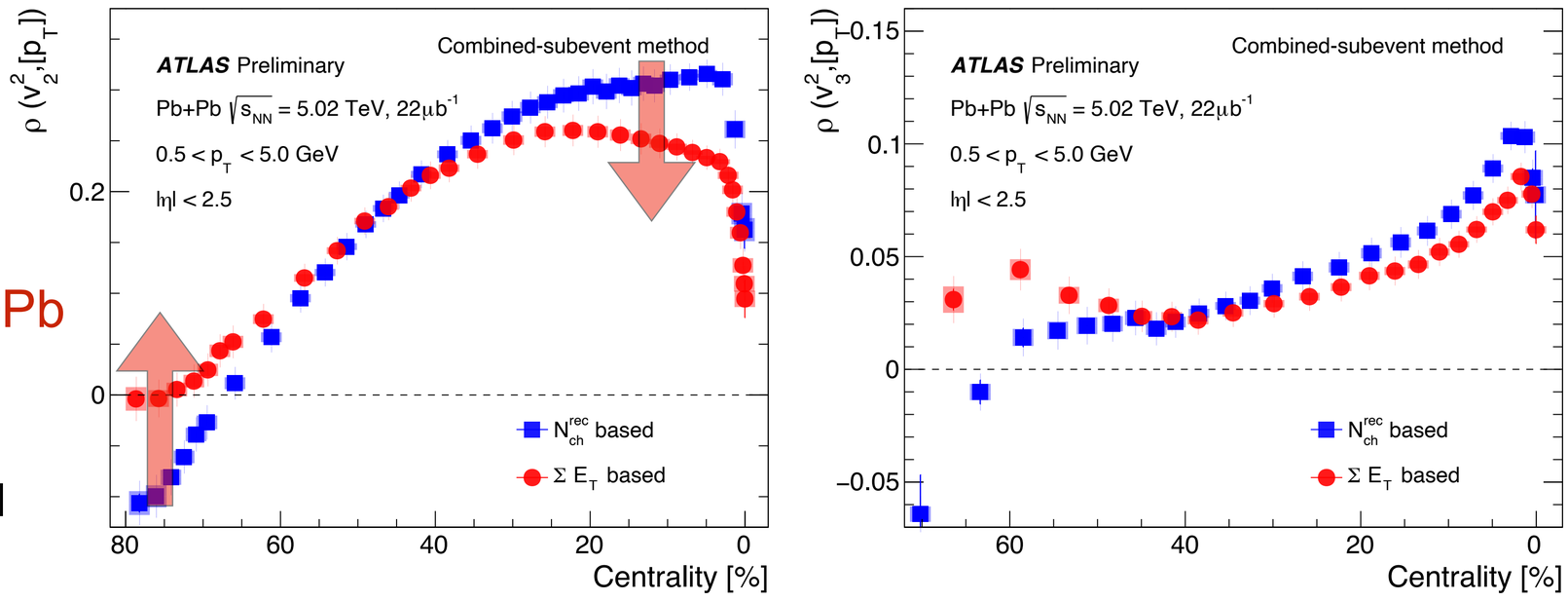

Centrality fluctuations in v_n-[p_T] correlation

- E_T and N_{ch} are mapped to centrality (based on E_T cuts)
- Significantly large centrality fluctuations in central and peripheral
- Less prominent in Xe+Xe but has similar trends - lower centrality resolution in Xe+Xe

Pb+Pb

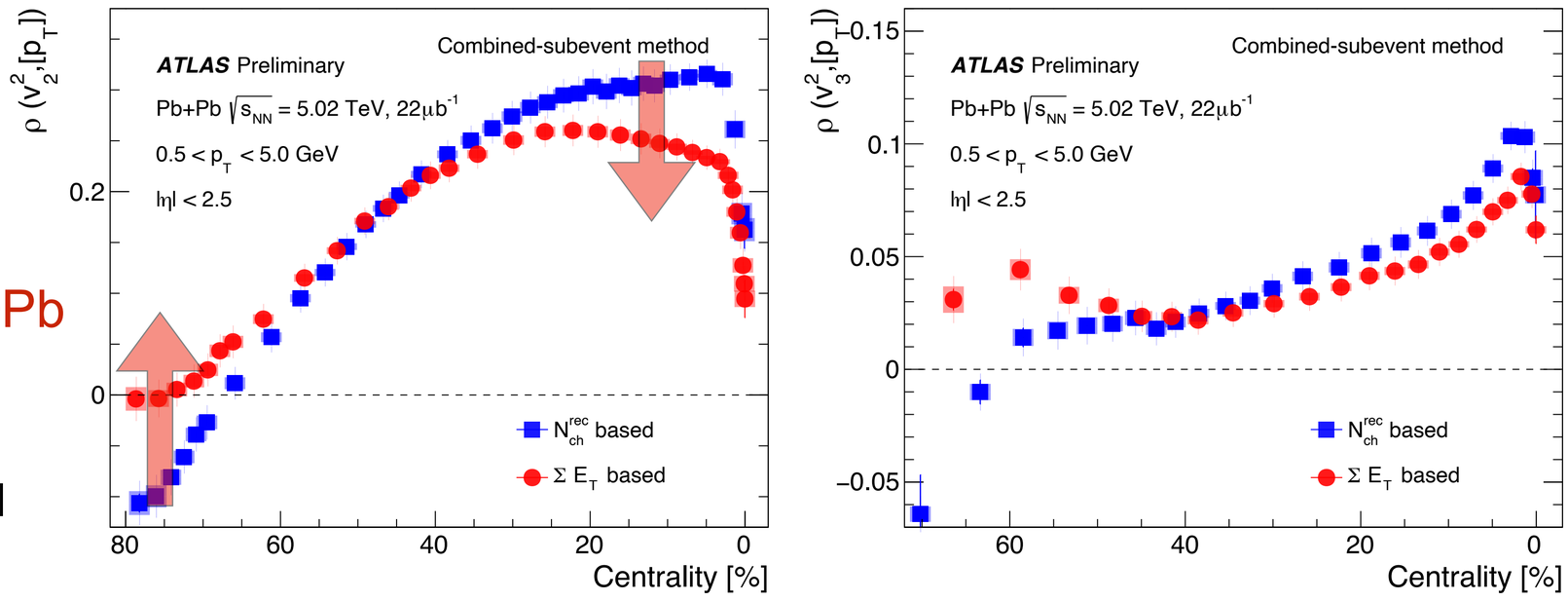

Xe+Xe

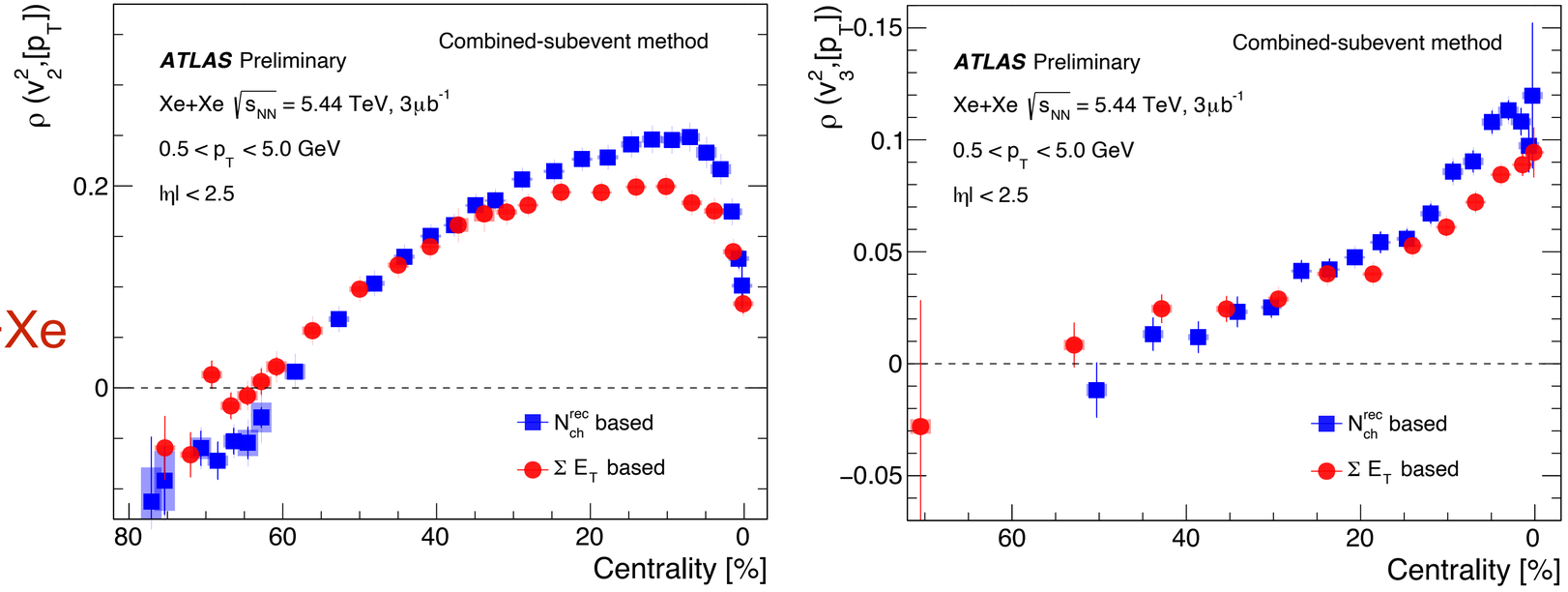

Comparison with Theory models

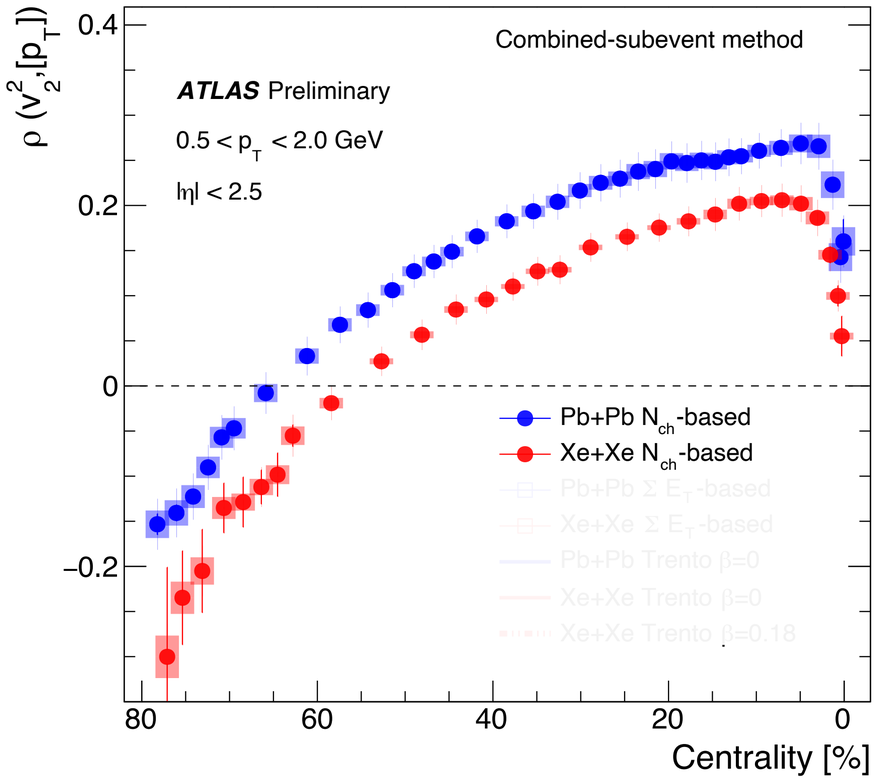

- ATLAS N_{ch}-based

Comparison with Theory models

Trento

G. Giacalone

Phys. Rev. C 102, 024901 (2020)

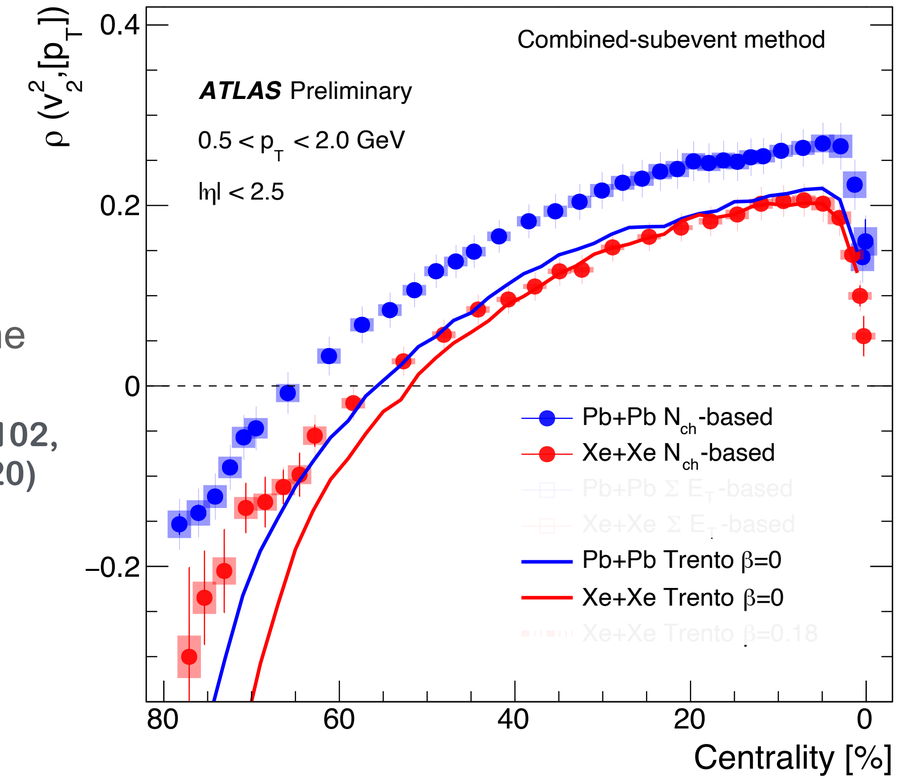

- ATLAS N_{ch}-based, Trento spherical
- Model captures centrality trends of data
- In contrast to data - little difference between Pb+Pb & Xe+Xe in the model

Comparison with Theory models

Trento

G. Giacalone

Phys. Rev. C 102, 024901 (2020)

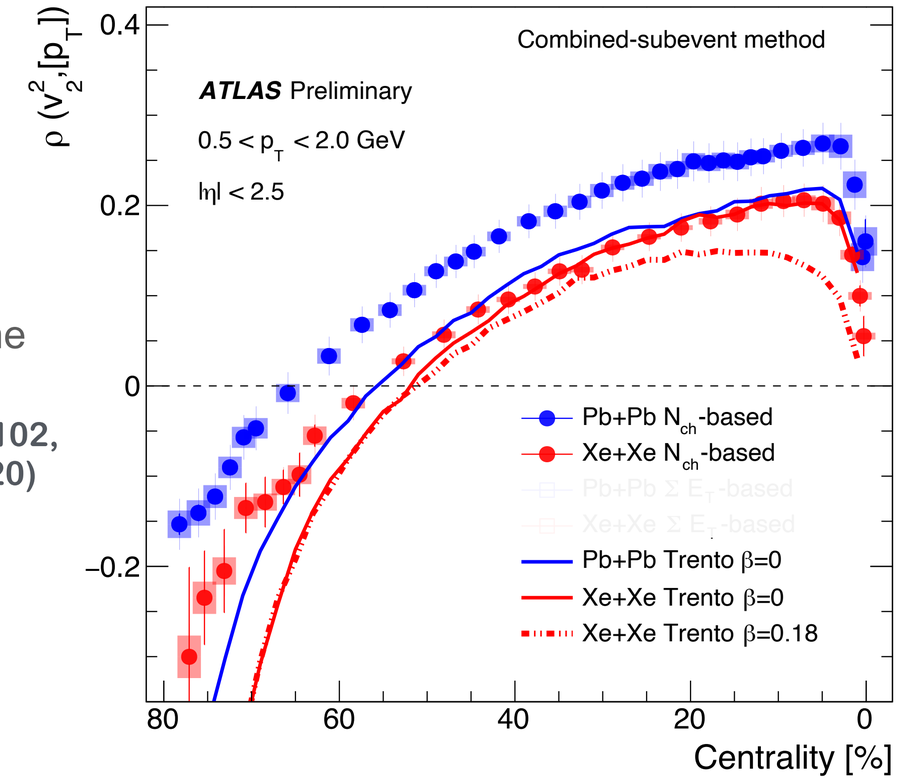

- ATLAS N_{ch}-based, Trento spherical, Trento deformed Xe+Xe
- Model captures centrality trends of data
- Deformed Xe+Xe - larger difference from Pb+Pb

Comparison with Theory models

Trento

G. Giacalone

Phys. Rev. C 102, 024901 (2020)

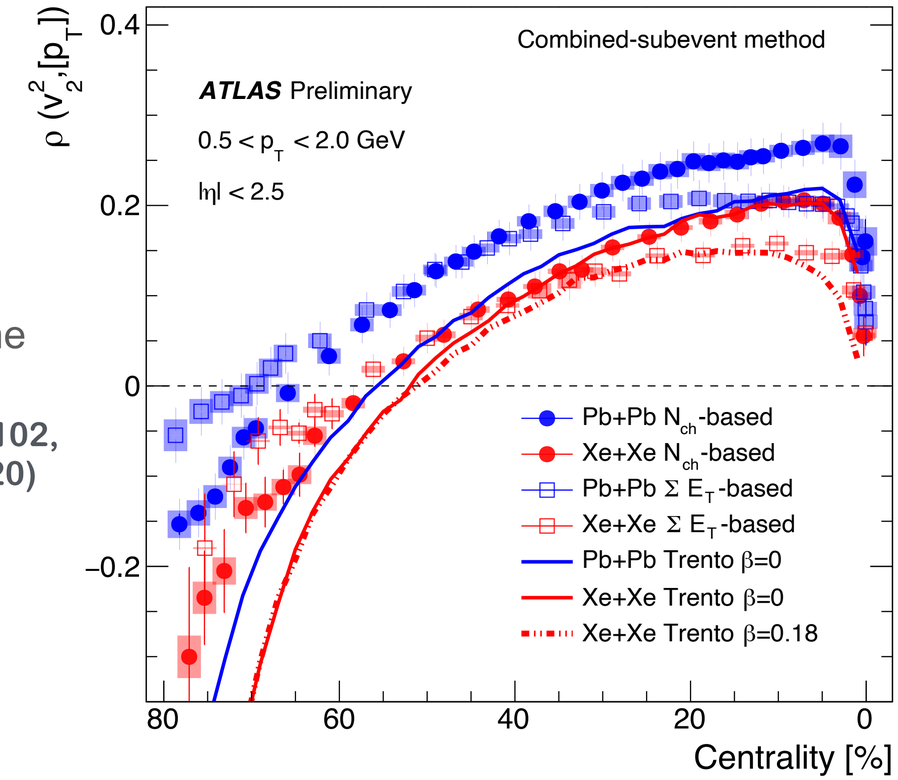

- ATLAS N_{ch}-based, Trento spherical, Trento deformed Xe+Xe, ATLAS E_T-based
- Results based on E_T - comparison to Trento better in central but worse in peripheral
- Trento model captures qualitative trends in data but cannot explain data quantitatively

Comparison with Theory models

G. Giacalone

Phys. Rev. C 102, 024901 (2020)

Trento

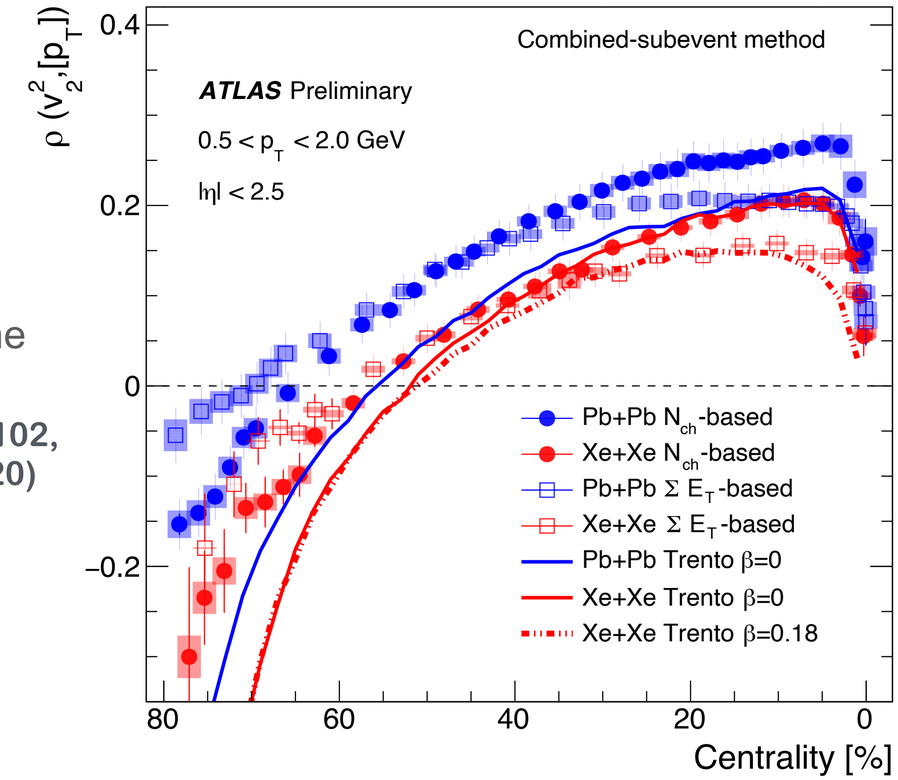

Trento+Hydro

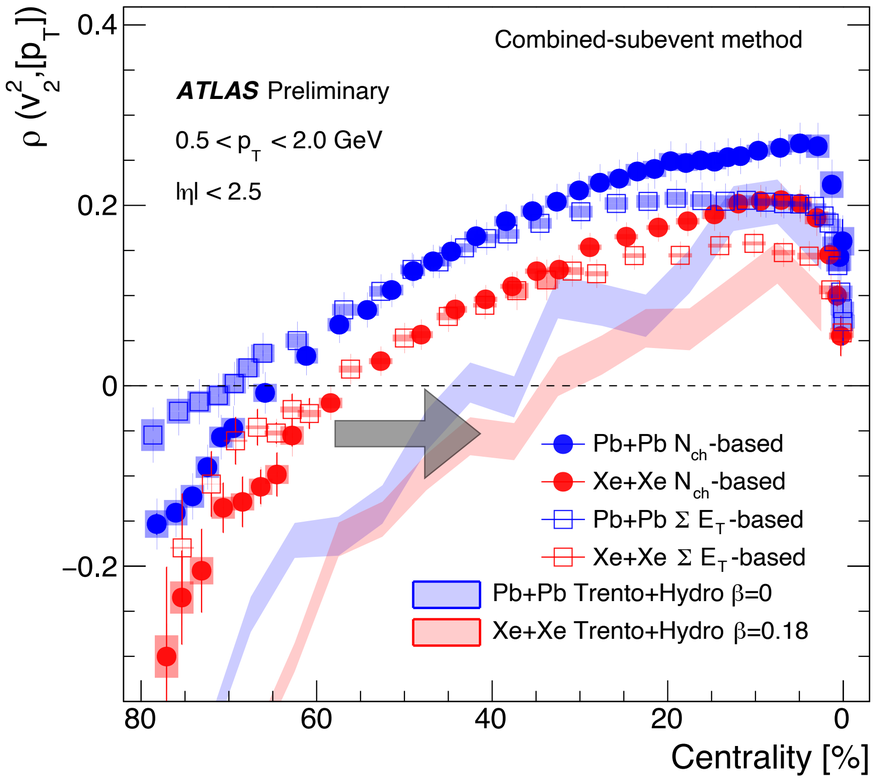

arXiv:2004.01765

- ATLAS N_{ch}-based, Trento spherical, Trento deformed Xe+Xe, ATLAS E_T-based
- Results based on E_T - comparison to Trento better in central but worse in peripheral
- Trento model captures qualitative trends in data but cannot explain data quantitatively

- Turning on final state hydrodynamic calculation
- Agreement with data becomes worse - shift of sign-change to lower centrality

Comparison with Theory models

Trento

G. Giacalone

Phys. Rev. C 102, 024901 (2020)

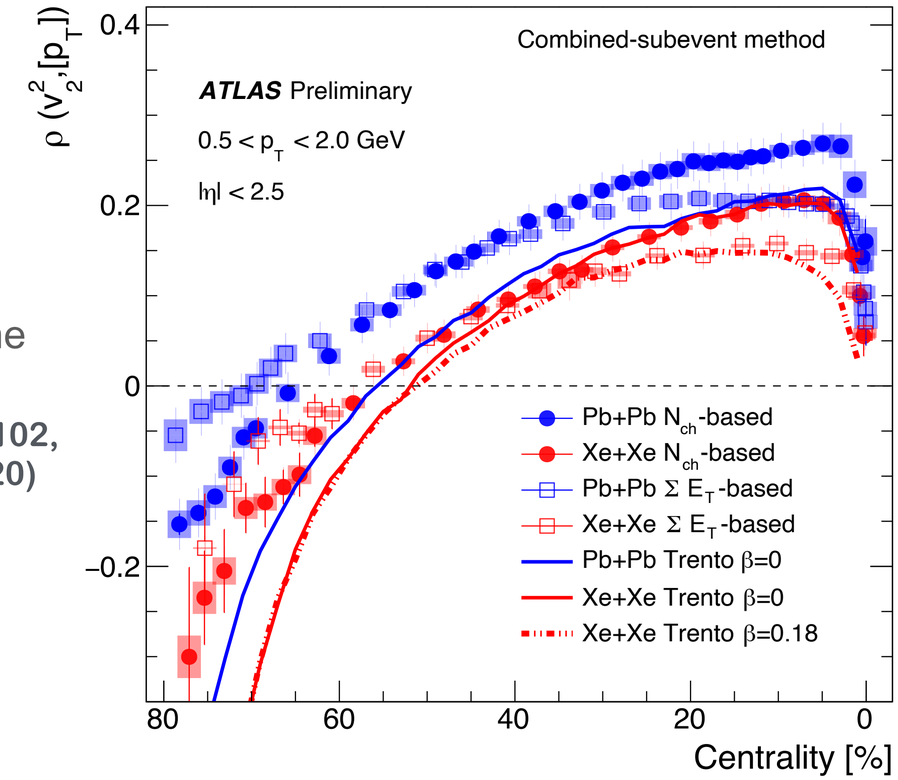

- ATLAS N_{ch}-based, Trento spherical, Trento deformed Xe+Xe, ATLAS E_T-based
- Results based on E_T - comparison to Trento better in central but worse in peripheral
- Trento model captures qualitative trends in data but cannot explain data quantitatively

CGC+Hydro

B. Schenke

Phys. Rev. C 102, 034905 (2020)

Phys. Rev. Lett. 125, 192301 (2020)

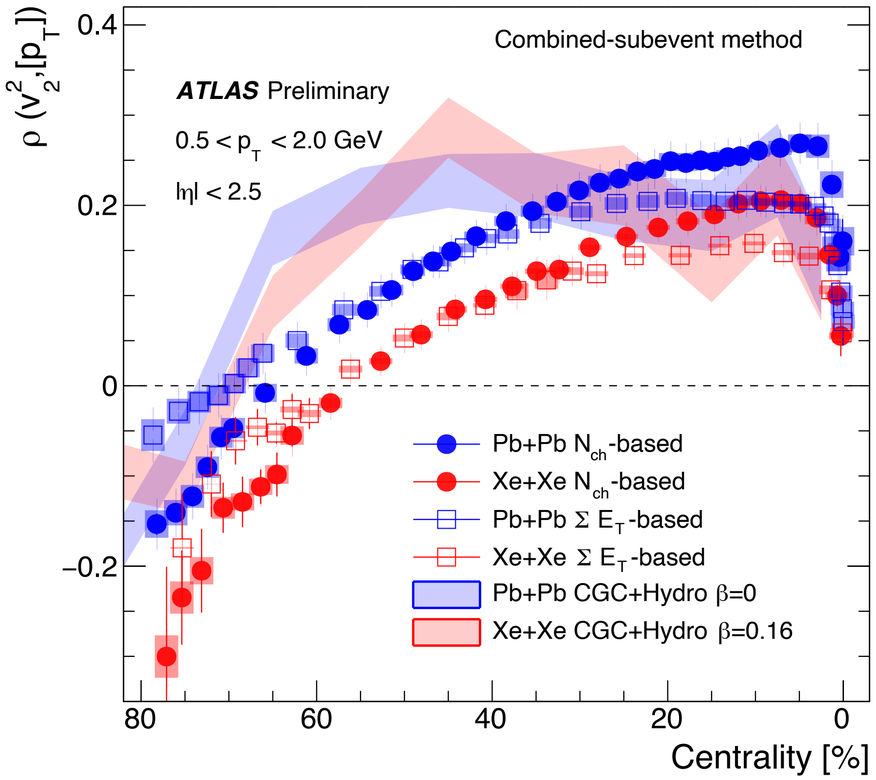

- Different hydrodynamic calculation with CGC initial conditions
- Does not see any significant difference between Pb+Pb and Xe+Xe
- Better agreement but still cannot describe data quantitatively

Summary

- Flow and mean-momentum correlations show strong system-size dependence
  - Smaller magnitude of ρ_{v_n} in XeXe for n=2
  - Larger magnitude in XeXe for n=3

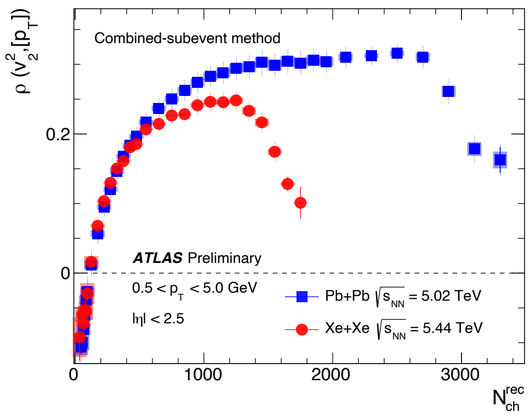

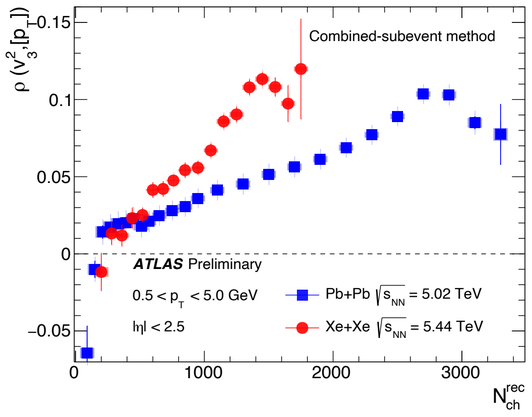

Summary

- Flow and mean-momentum correlations show strong system-size dependence
  - Smaller magnitude of ρ_{v_n} in XeXe for n=2
  - Larger magnitude in XeXe for n=3
- Sensitive to p_T and η ranges
  - Increase in ρ_{v_n} with more high p_T particles
  - Larger variances for smaller η range (|η|<1)
  - Covariance depends weakly on η range selection

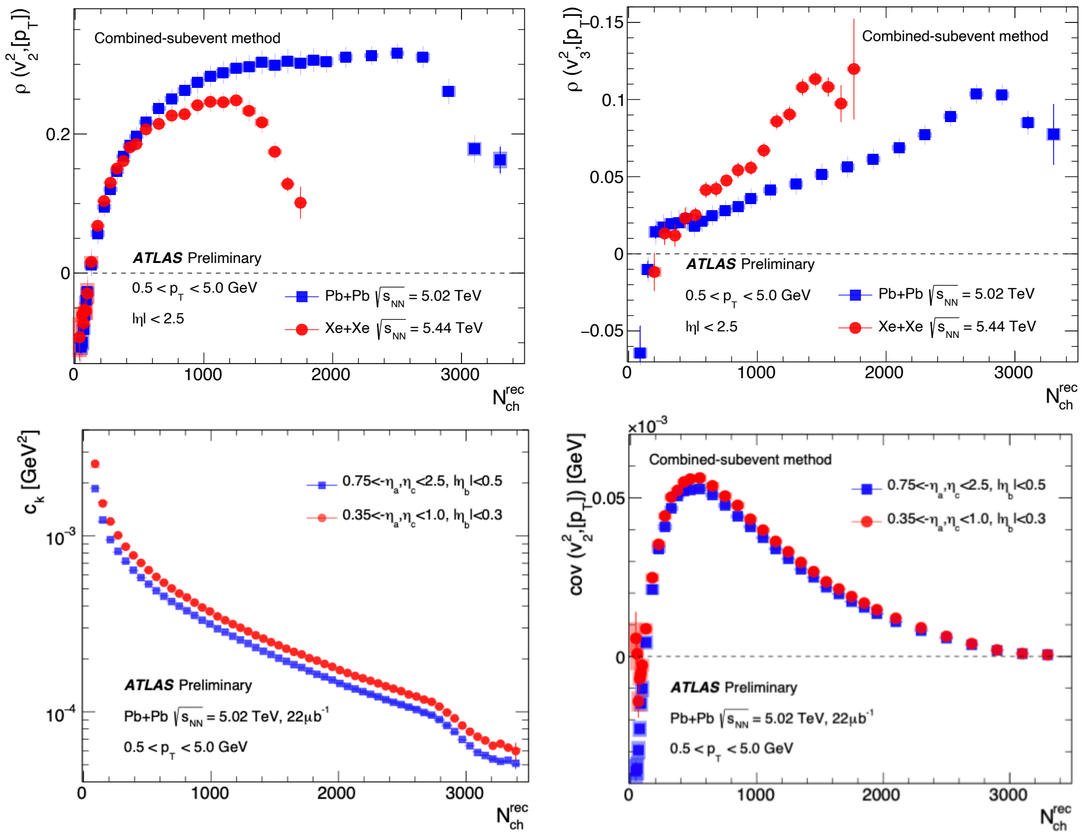

Summary

- Flow and mean-momentum correlations show strong system-size dependence
  - Smaller magnitude of ρ_{v_n} in XeXe for n=2
  - Larger magnitude in XeXe for n=3
- Sensitive to p_T and η ranges
  - Increase in ρ_{v_n} with more high p_T particles
  - Larger variances for smaller η range (|η|<1)
  - Covariance depends weakly on η range selection
- Significant Centrality fluctuations - N_{ch} vs E_T binnings
- Compared results with theory
  - Trento model captures qualitative trends in data
  - Models do not explain the measurements quantitatively

Poster by Somadutta Bhatta - Tuesday 12th

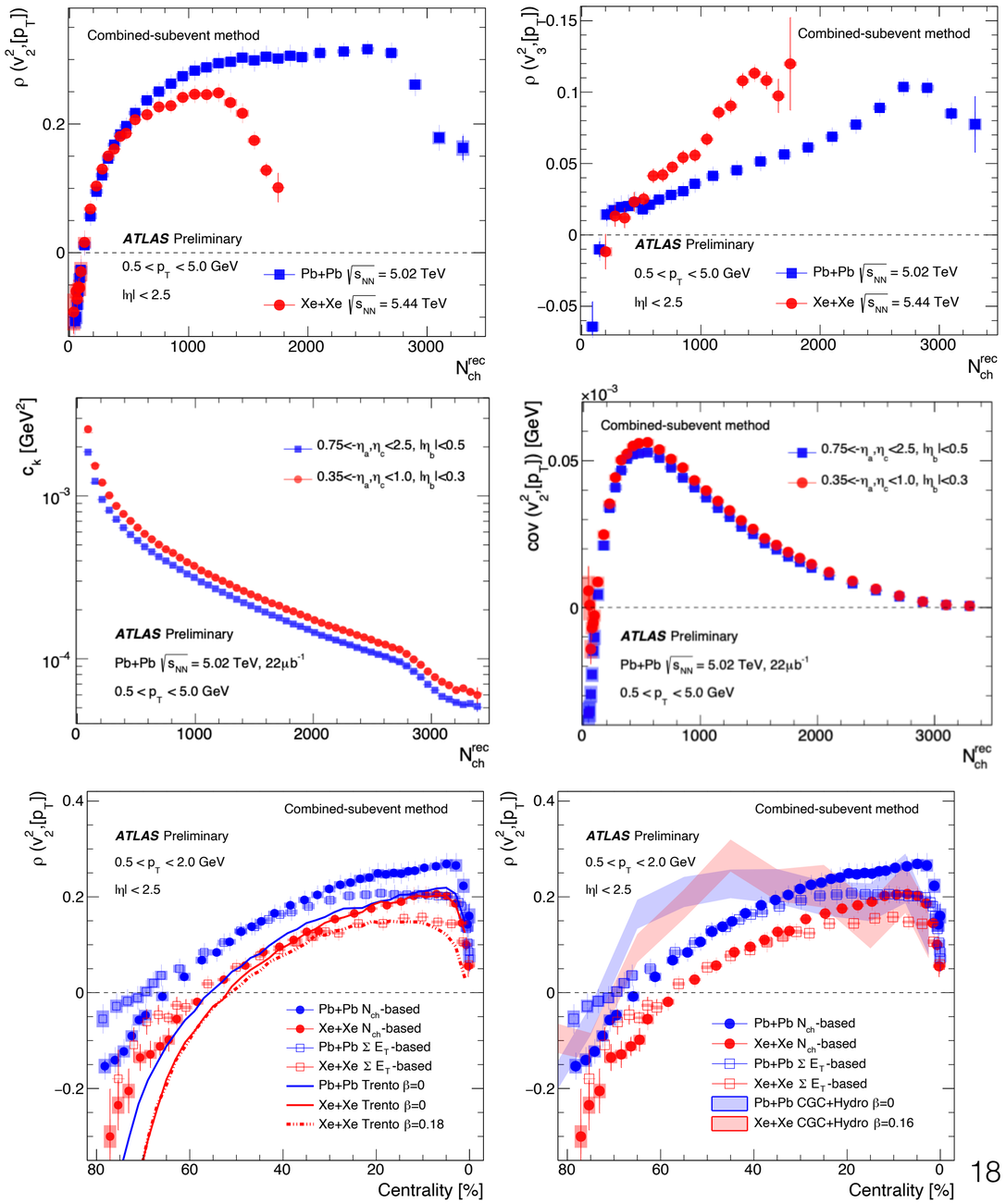

Backup

Observable

- Pearson's Correlation coefficient

$$\rho(v_n\{2\}^2, [p_T]) = \frac{\mathrm{cov}(v_n\{2\}^2, [p_T])}{\sqrt{\mathrm{var}(v_n\{2\}^2)c_k}},$$

$$\delta p_T = p_T - [p_T]$$

$$\mathrm{cov}(v_n\{2\}^2, [p_T]) = \langle\langle v_n^2 \delta p_T \rangle\rangle \ , \ \mathrm{var}(v_n\{2\}^2) = \langle v_n^4 \rangle - \langle v_n^2 \rangle^2 \ , c_k = \langle\langle \delta p_T \delta p_T \rangle\rangle$$

- Covariance - from three methods
  - Standard - full η-range |η|<2.5
  - 2-SE - A and C with Δη=1.5, [pT] from A+C
  - 3-SE - A and C with Δη=1.5, [pT] from B (|η| < 0.5)

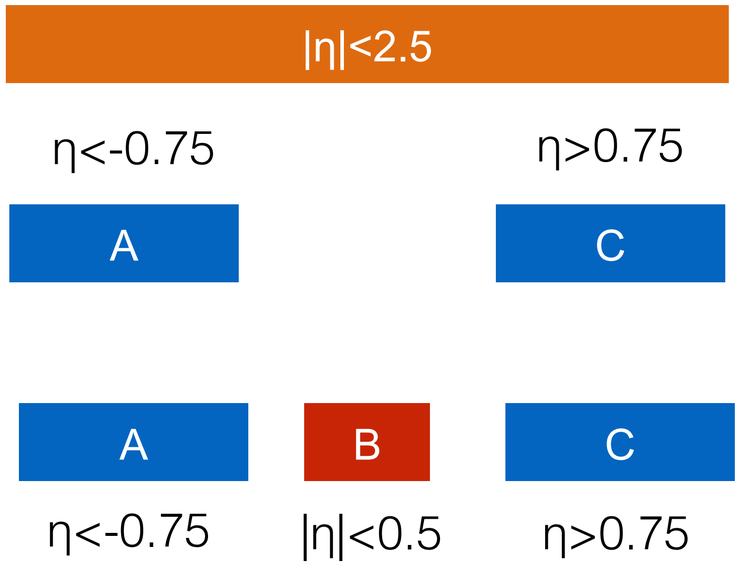

- C_k - Standard - |η|<2.5

- Variance v_n : $\mathrm{var}(v_n\{2\}^2) = c_n\{4\}_{\mathrm{standard}} + c_n\{2\}^2_{\mathrm{two-sub}}$

Other physics sources

- Non-flow
  - Short-range non-flow (single jets, resonance decays, etc.) suppressed in subevent methods
  - Long-range non-flow (dijets) - contribute to atmost 2-subevents and scale as 1/sqrt(N)
- Eta-dependence of vn
  - vn smaller at larger eta
  - Stronger dependence in peripheral
- vn decorrelation
  - Smaller signal at larger deta
  - Stronger in central and peripheral
- Flow and non-flow depends on η range, location of subevents and gap.

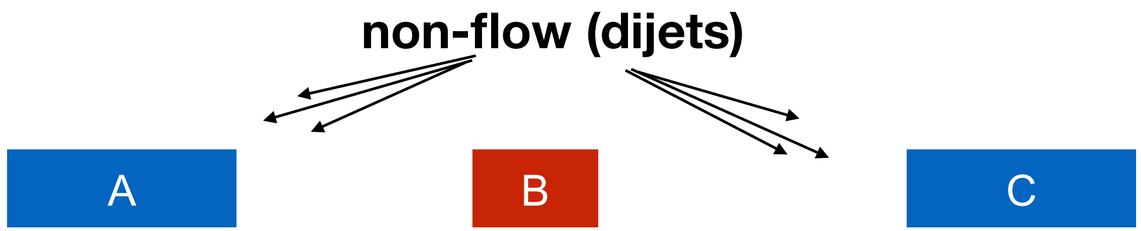

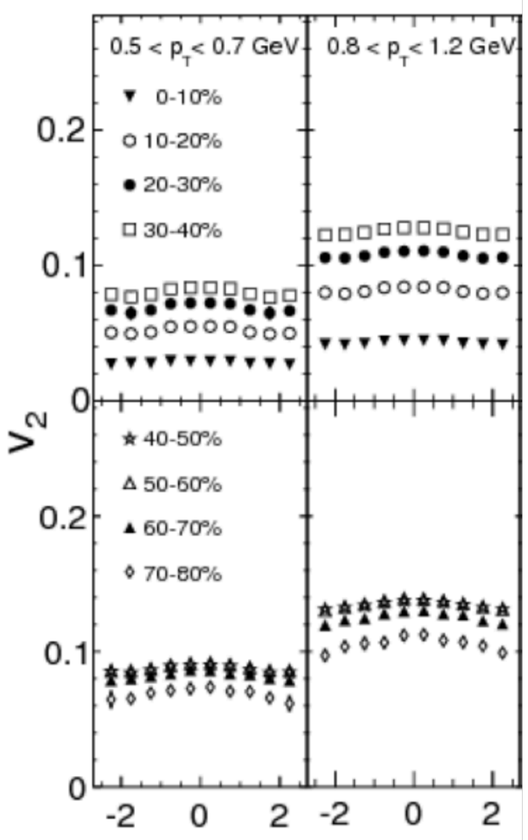

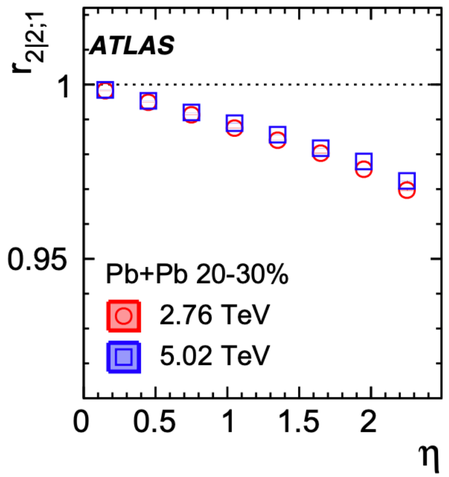

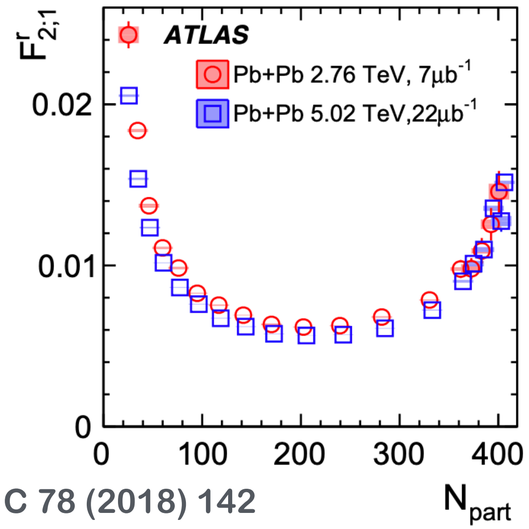

Eur. Phys. J. C 78 (2018) 142

Comparisons - Xe+Xe vs Pb+Pb

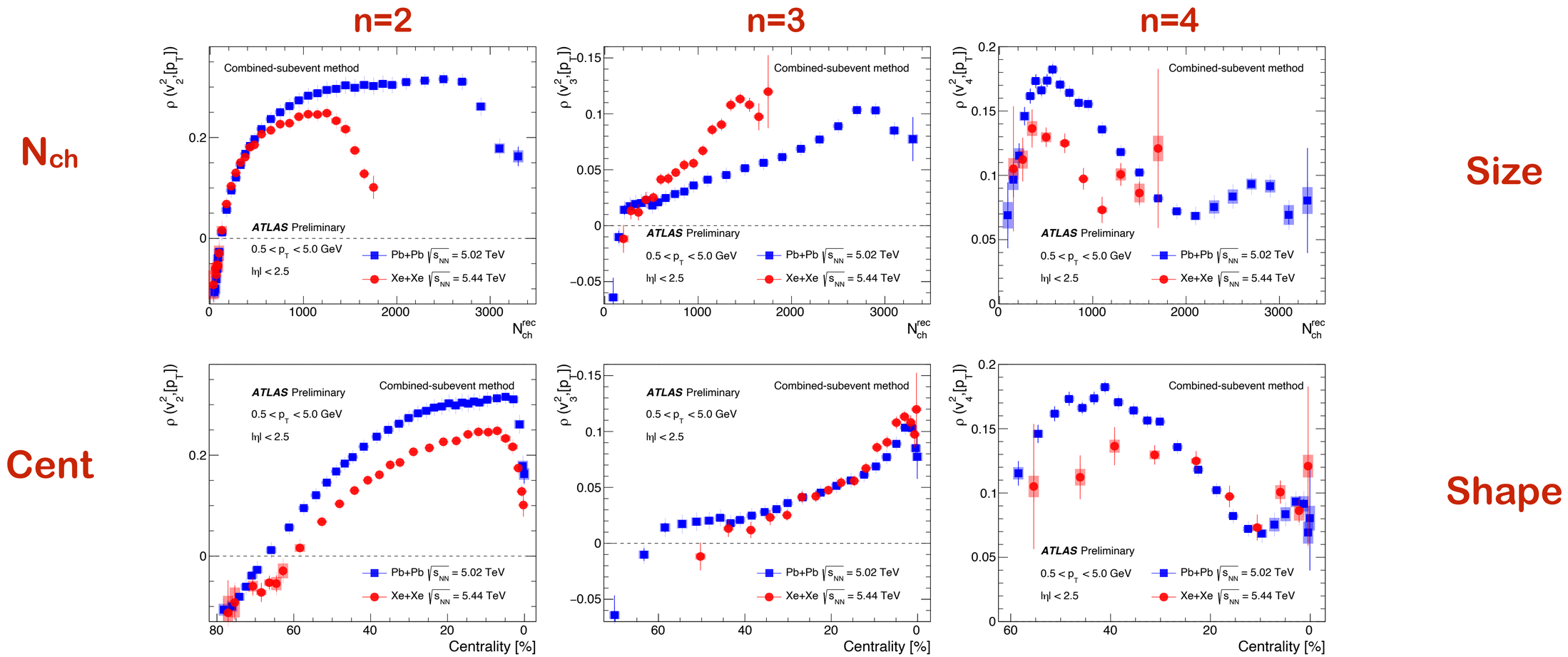

- Both Xe+Xe and Pb+Pb go -ve in very low Nch for n=2
- Smaller magnitude in Xe+Xe for n=2 & n=4
- Larger magnitude in Xe+Xe for n=3 due to larger fluctuations in smaller system
- As a function of centrality, ρ_2 is smaller in Xe+Xe but ρ_3 and ρ_4 are comparable

η-dependence in Pb+Pb

Cov

ρ

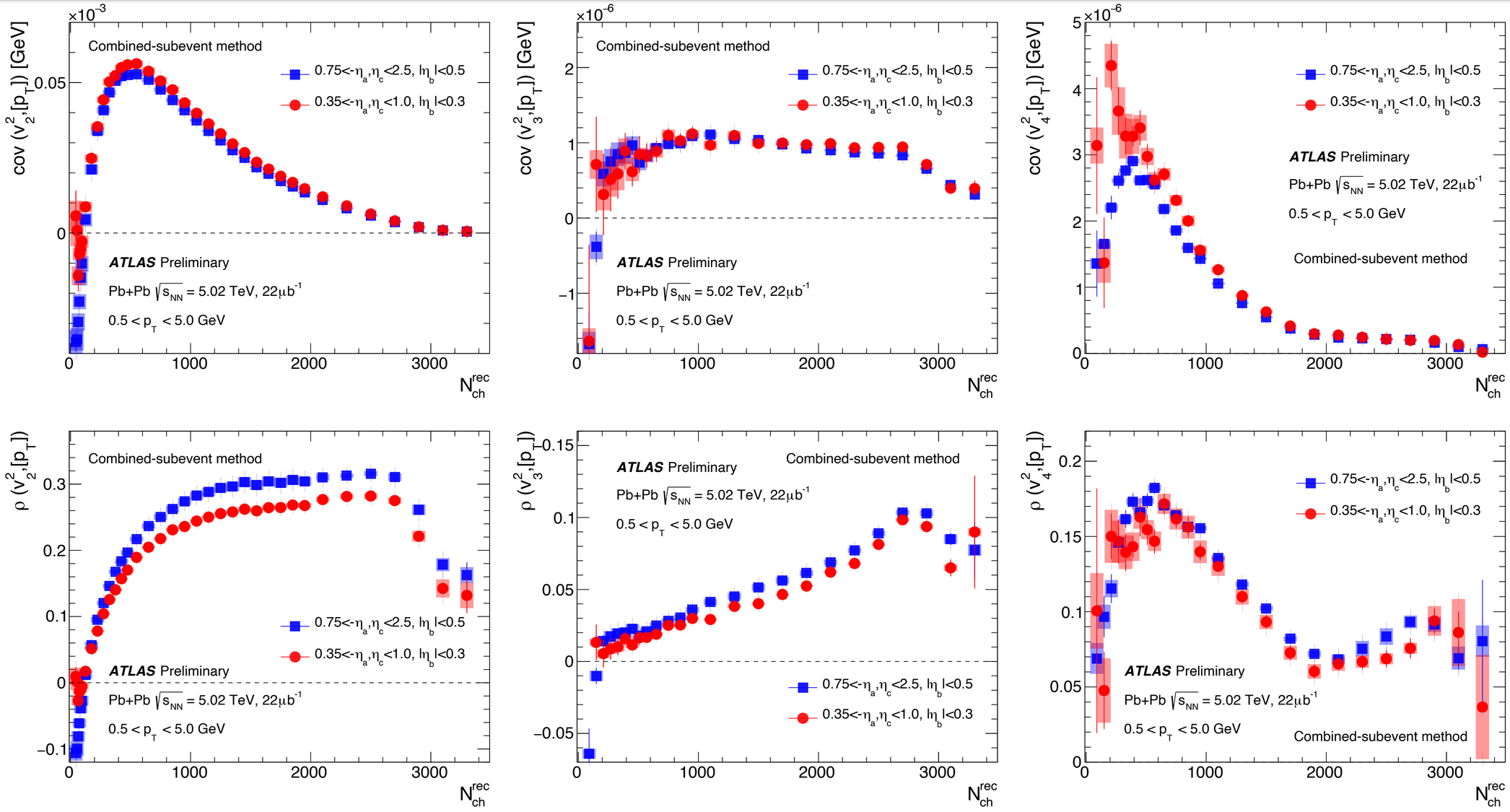

- Covariances show good agreement between eta-ranges except for n=4 at low N_{ch}
- ρ is systematically smaller for $|\eta| < 2.5$ due to smaller c_k and $var(v_n)$

Centrality fluctuations in v_n-[p_T] correlation

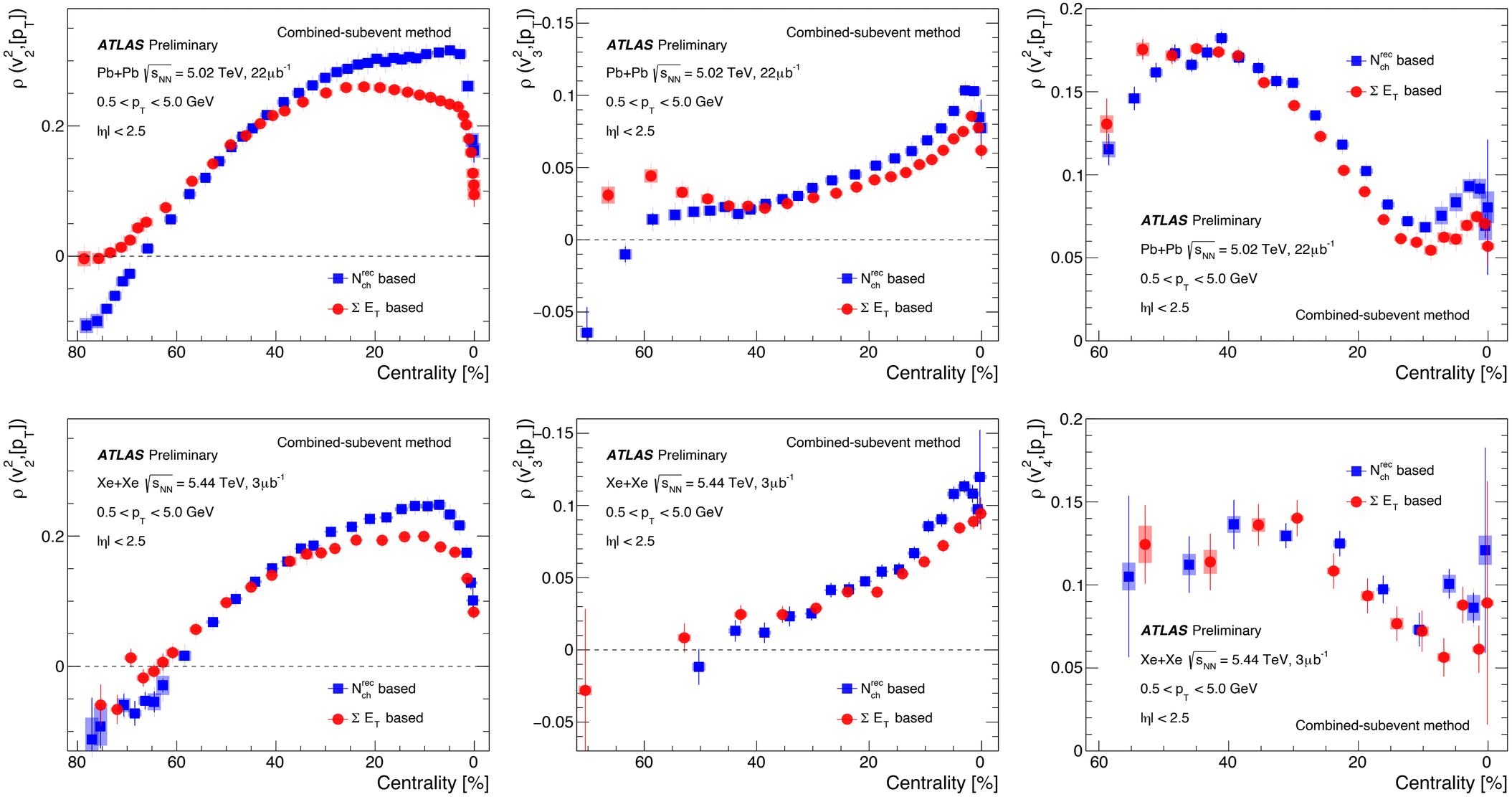

- E_T and N_{ch} are mapped to centrality (based on E_T cuts)
- Large influences of centrality fluctuations for all harmonics
- Trends similar in Pb+Pb and Xe+Xe

Comparison with Theory

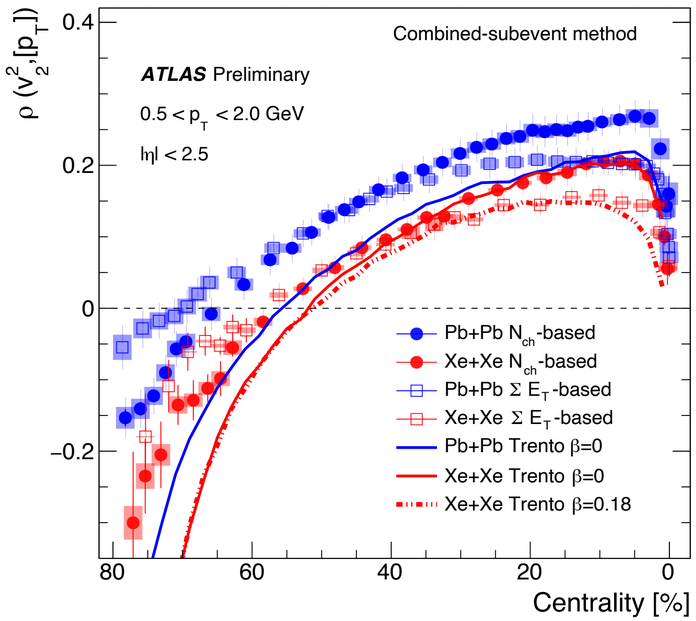

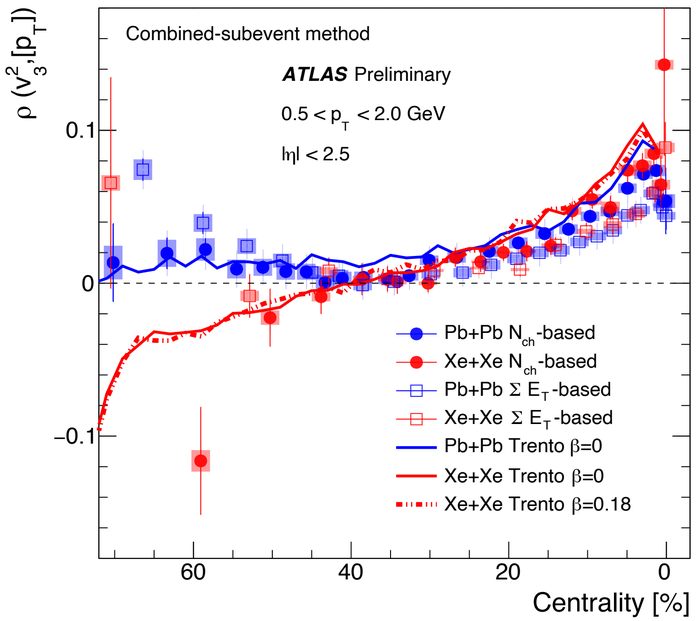

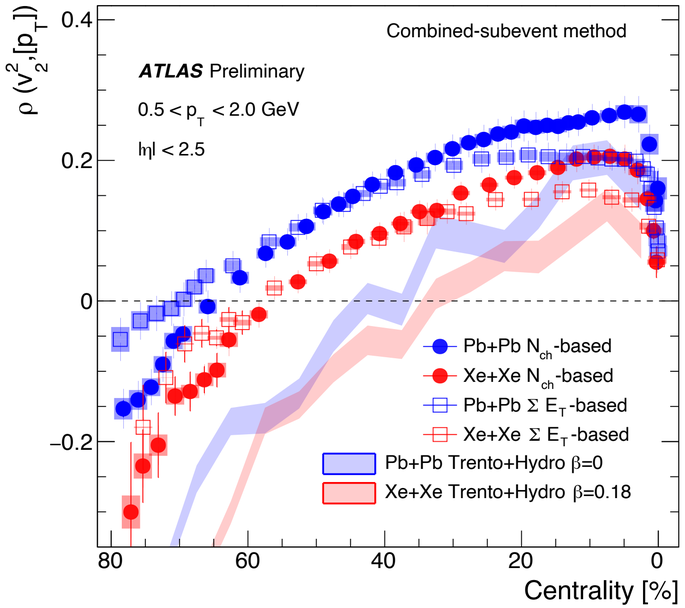

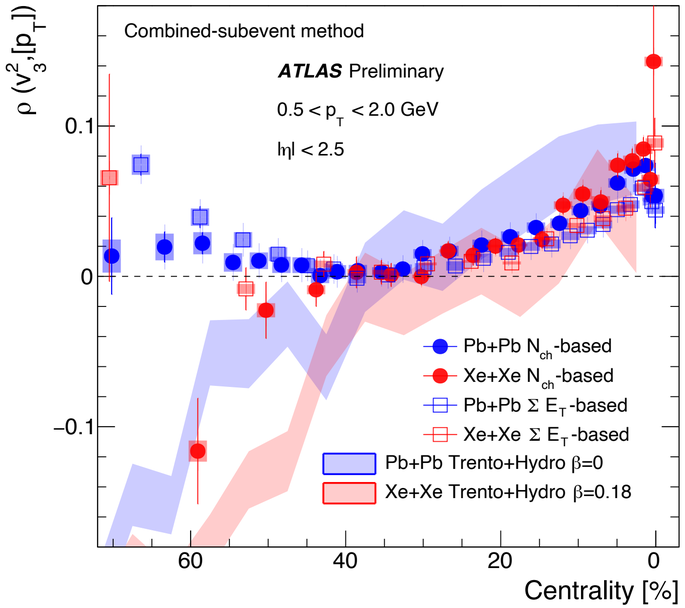

Comparison with Theory

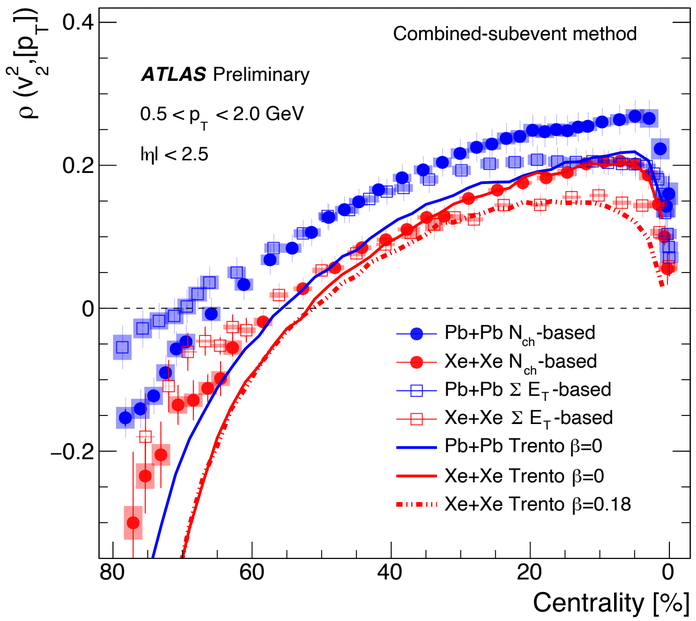

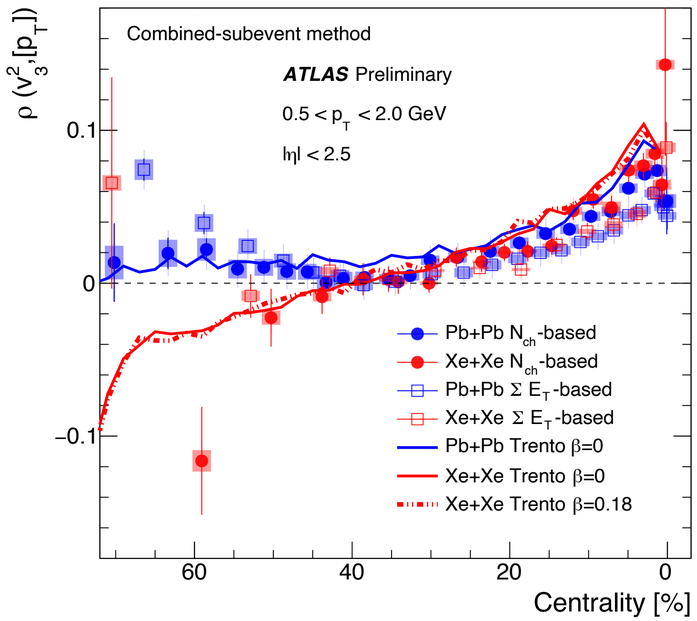

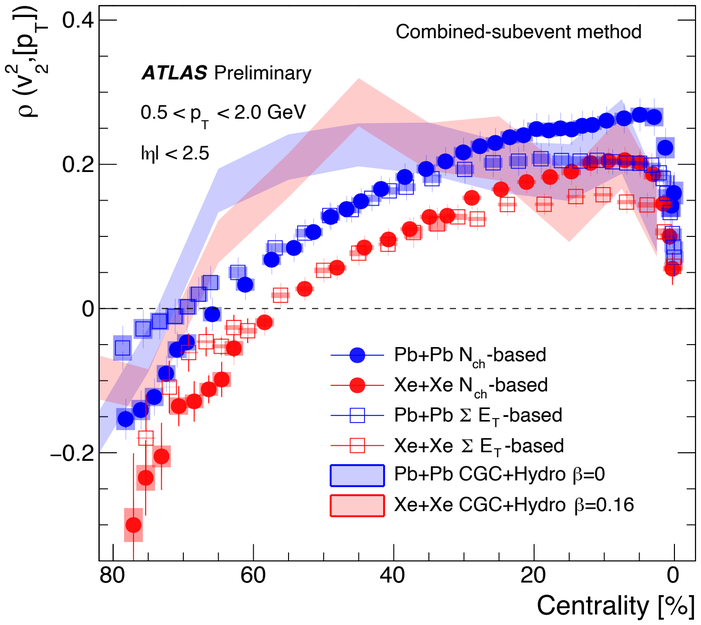

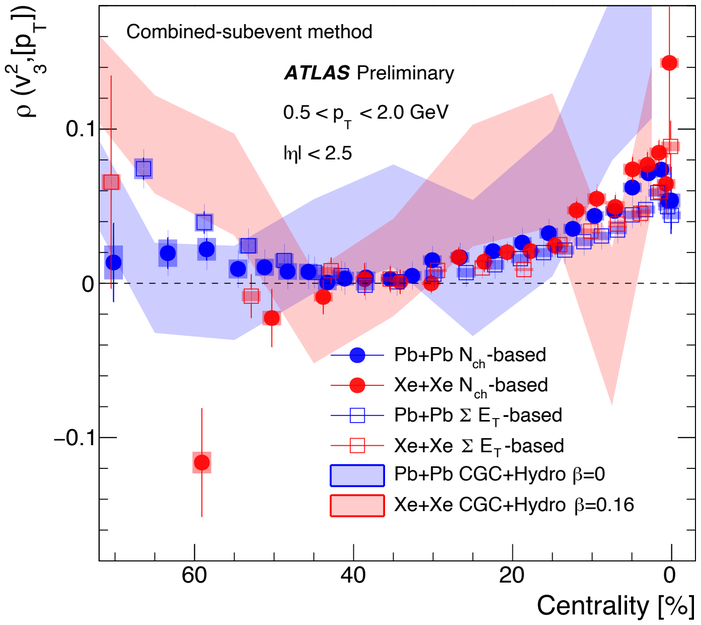

Comparison of cov(v_n^2,[p_T]) - subevents methods

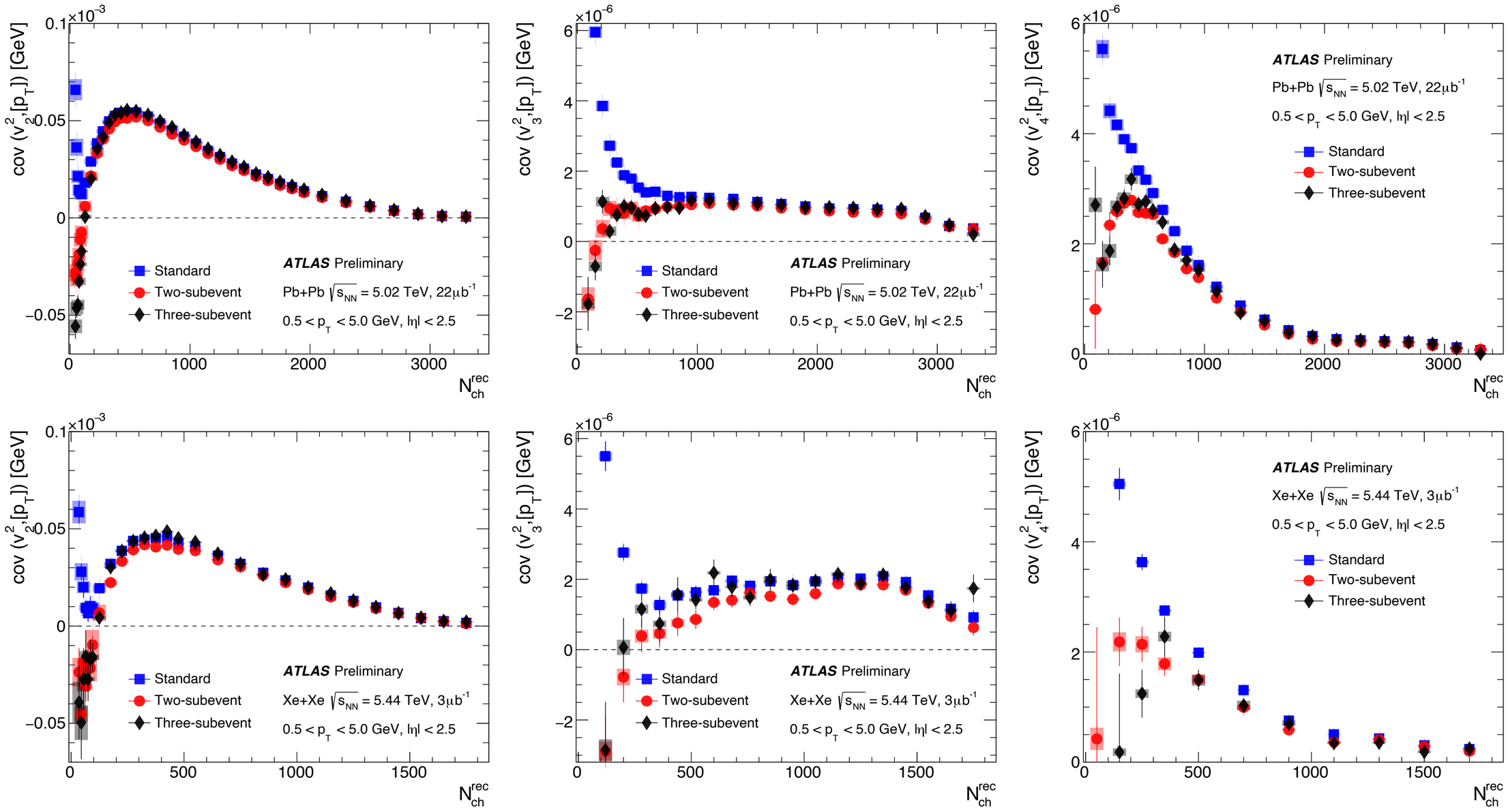

Comparison of $\rho(v_n^2,[p_T])$ - subevents methods